

Buckling and vibration analyses of MGSST double-bonded micro composite sandwich SSDT plates reinforced by CNTs and BNNTs with isotropic foam & flexible transversely orthotropic cores

M.Mohammadimehr*, E. Shabani Nejad and M. Mehrabi

Department of Solid Mechanics, Faculty of Mechanical Engineering, University of Kashan, Kashan, P. O. Box: 87175-53153, Iran

(Received October 3, 2017, Revised December 23, 2017, Accepted December 26, 2017)

Abstract. Because of sandwich structures with low weight and high stiffness have much usage in various industries such as civil and aerospace engineering, in this article, buckling and free vibration analyses of coupled micro composite sandwich plates are investigated based on sinusoidal shear deformation (SSDT) and most general strain gradient theories (MGSST). It is assumed that the sandwich structure rested on an orthotropic elastic foundation and make of four composite face sheets with temperature-dependent material properties that they reinforced by carbon and boron nitride nanotubes and two flexible transversely orthotropic cores. Mathematical formulation is presented using Hamilton's principle and governing equations of motions are derived based on energy approach and applying variation method for simply supported edges under electro-magneto-thermo-mechanical, axial buckling and pre-stresses loadings. In order to predict the effects of various parameters such as material length scale parameter, length to width ratio, length to thickness ratio, thickness of face sheets to core thickness ratio, nanotubes volume fraction, pre-stress load and orthotropic elastic medium on the natural frequencies and critical buckling load of double-bonded micro composite sandwich plates. It is found that orthotropic elastic medium has a special role on the system stability and increasing Winkler and Pasternak constants lead to enhance the natural frequency and critical buckling load of micro plates, while decrease natural frequency and critical buckling load with increasing temperature changes. Also, it is showed that pre-stresses due to help the axial buckling load causes that delay the buckling phenomenon. Moreover, it is concluded that the sandwich structures with orthotropic cores have high stiffness, but because they are not economical, thus it is necessary the sandwich plates reinforce by carbon or boron nitride nanotubes specially, because these nanotubes have important thermal and mechanical properties in comparison of the other reinforcement.

Keywords: buckling and free vibration analyses; double-bonded micro composite sandwich plates; most general strain gradient theory; sinusoidal shear deformation plate theory; orthotropic foundation

1. Introduction

In the last years, sandwich structures with high stiffness and low weight have much usage in various industries (Botshekanan Dehkordi *et al.* 2013). Usually, these structures are made of two stiff face sheets and a soft core such as flexible transversely materials and they used to analyze the microplates (Batra *et al.* 2008a), microbeams, microbars (Reissner (1948)) and microshells (Batra *et al.* (2008b)) that they have found many applications in micro-electro-mechanical systems (MEMS), nano-electro-mechanical systems (NEMS) and atomic force microscopes (AFMs). Recently, the composite materials are used to build the sandwich skins (Ke *et al.* 201), therefore because of increasing the structures stiffness, it is necessary to partake reinforcement (Wang and Hu 2005). Carbon and boron nitride nanotubes (CNTs and BNNTs) are new types of advanced reinforcement that they have promising application in polymer composites due to their attractive mechanical, thermal, magnetic and electrical properties

(Lau *et al.* 2002, Lei *et al.* 2013). Thus, these nanotubes lead to enhance the tensile strength and elastic modulus (Thostenson 2001). Kaghazian *et al.* (2017) researched about free vibration analysis of a piezoelectric nano beam based on Euler-Bernoulli beam theory (EBT). They showed that increasing a positive voltage leads to decrease the natural frequencies, while increasing a negative voltage increases them. A size dependent continuum model developed by Rouhi *et al.* (2016) in order to study vibration analysis of nano cylindrical shells based on the first order shear deformation theory (FSDT). They concluded that the size-dependent behaviors of nano cylindrical shell intensify and increase as the surface residual tension increases. In order to compare the obtained results from experimental and numerical investigation, Ferreira *et al.* (2013) presented a layer-wise finite element (FE) model for the analysis of sandwich laminated plates and showed that there is a good agreement between their model and experimental results. Xu *et al.* (2017) considered vibration behavior of single-layer graphene sheets (SLGSs) based on nonlocal continuum orthotropic plate model. They predicted that a thicker SLGS produces a higher natural frequency if the SLGS density, remain unchanged. Wang *et al.* (2017) investigated the micro structure dependent axisymmetric

*Corresponding author, Associate Professor
E-mail: mmohammadimehr@kashanu.ac.ir

large deflection bending of pressure loaded circular FG microplates. Their obtained results demonstrated that the size effect on the bending deflection of simply supported boundary conditions was not important against clamped boundary conditions. Using FE method, Mohammadimehr and Alimirzaei (2016a) studied nonlinear static and free vibration response of EBT composite beam reinforced by functionally graded single walled carbon nanotubes (FG-SWCNTs) with initial geometrical imperfection uniformly load. They showed that at the specified value of thickness-to-length ratio, the natural frequencies ratio enhances when the values amplitude of waviness increases. Civalek *et al.* (2009) studied static analysis of CNT using nonlocal EBT. They used differential quadrature method (DQM) for bending analysis of numerical solution of CNTs. Ergun *et al.* (2016) investigated buckling and free vibration analyses of hybrid composite beams having different span lengths and orientation angles subjected to different impact energy levels and compared with each other for different span lengths, orientation angles and impact levels. Ghorbanpour Arani and Zamani (2017) presented electro-mechanical bending behavior of sandwich nanoplate with functionally graded porous core and piezoelectric face sheets. Vlasov's model foundation is utilized to model the silica Aerogel foundation. Two functions are considered for nonuniform variation of material properties of the core layer along the thickness direction such as Young's modulus, shear modulus, and density. Chen and Feng (2017) established a dynamic modelling of a thin laminated plate subjected to in-plane excitation. Farajpour *et al.* (2017) proposed thermal environment buckling, vibration and smart control of microtubules (MTs) and piezoelectric nano shells. They showed that applied electric voltage can be used as an effective controlling parameter for the vibration and buckling of MTs. Based on FSDT and using FE method, Zhu *et al.* (2012) presented static bending and free vibration analyses of composite plates reinforced by various distributions of SWCNTs. The results of their study investigated that the effect of CNTs volume fraction on the central axial stress can be neglected. Bahadori and Najafzadeh (2015) examined the dynamic response of two dimensional FG cylindrical shell. They demonstrated that when the power law index in z direction increases, the natural frequencies increase faster. Miraslani *et al.* (2017) illustrated the mechanical instability and free vibration of FG micro plate based on MSGT and using spline finite strip method. Yan and Liew (2016) used analytically and experimentally methods for ultimate strength behaviors of steel-concrete-steel (SCS) sandwich plates. They depicted that for the full and partial composite SCS sandwich plate, increasing the strength of concrete core increases first and second peak resistance. Dai *et al.* (2016) predicted the nonlinear forced vibration analysis of a cantilevered nanobeam. They demonstrated that the combined effects of the residual stress and aspect ratio on the maximum amplitude of the nanobeam may be pronounced. Mirjavadi *et al.* (2017) examined free vibration and thermal buckling behaviors of axially functionally graded (AFG) nanobeam under thermal environment effect and various boundary conditions based on EBT and Eringen's nonlocal elasticity

theory. Their results demonstrated that enhancing thermal expansion coefficient increases the dimensionless natural frequency and critical buckling load of AFG nanobeam. Mohammadimehr and Mehrabi (2017) applied generalized DQM to analyze stability and free vibration analyses of double-bonded micro composite sandwich moderately thick walled cylindrical shells conveying fluid based on MCST. Their results showed that with increasing flow velocity in the flow-conveying micro structures, the system was unstable. Robin *et al.* (2017) considered free vibration analysis of 3D structured beams based on FEM and experimental tests. They compared and validated the numerical results with experimental test and showed that the resonant frequencies generally increase due to corrugated shape. Shen *et al.* (2017) studied small and large amplitude vibrations of thermally post-buckled sandwich plates reinforced by CNTs. The results of their research illustrated that the core-to-face sheets thickness ratio lead to enhance the structure stiffness. Thus, the vibration characteristics increased when increased the thickness ratio. Li *et al.* (2016) developed static and free vibration analyses of composite sandwich structures with multi-layer cores using layer-wise/Solid-element (LW/SE) method. Bahaadini *et al.* (2017) developed dynamic structural instability of flow-conveying cantilever nanotubes resting on a visco-Pasternak medium. Their results showed that critical flow velocity decreased by increasing the value of the distributed compressive tangential load. Swaminathan and Sangeetha (2017) presented a review of applications, various mathematical idealizations of materials, modeling techniques and solution method that are adopted for the thermal analysis of FG plates.

In the present work, using most general strain gradient theory (MGSST), the free vibration and buckling analyses of double-bonded micro composite sandwich plates rested in an orthotropic foundation are investigated based on sinusoidal shear deformation theory (SSDT). This system is simulated with four composite temperature-dependent face sheets reinforced by CNTs (upper micro sandwich plate) and BNNTs (lower micro sandwich plate) and two flexibly transversely orthotropic cores. Governing equations of motions are obtained using energy method. It is noted that in the previous study, usually the MGSST used for the simple geometry such as beam and CT plates, while in this article this theory are applied for the higher order plates. Also, this micro structure is considered as coupled sandwich system with temperature-dependent material properties under various multi-physics fields that they are the other novelty of present work.

2. Geometry and simulation

A schematic of double-bonded micro composite sandwich SSDT plates reinforced by CNTs and BNNTs with length a , width b and thickness h rested in an orthotropic elastic foundation under electro-magneto-thermo-mechanical loadings, pre-stresses load and two-dimensional (2D) axial buckling load are shown in Fig. 1.

It is assumed that the cores of sandwich micro plates are made of transversely flexible orthotropic cores with thickness

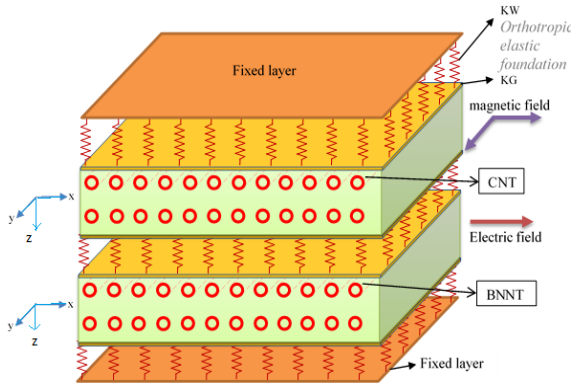


Fig. 1 Schematic of double-bonded micro composite sandwich SSDT plates reinforced by CNTs and BNTs rested in an orthotropic foundation under various multi-physic fields

Table 1 Mechanical properties of orthotropic core with $\nu_1=0.25, \nu_2=0.30$ (Chakrabarti *et al.* 2007)

E_{11}^{Cor} (GPa)	E_{22}^{Cor} (GPa)	G_{12}^{Cor} (GPa)	G_{13}^{Cor} (GPa)	G_{23}^{Cor} (GPa)	α_{11}^{Cor} ($10^{-6} / K$)	α_{22}^{Cor} ($10^{-6} / K$)
7.347	8.816	3.159	4.218	4.197	3.458	5.168

Table 2 Mechanical properties of SWCNTs (10,10) with $\nu=0.175$ (Mohammadimehr *et al.* 2016c, Zhu *et al.* 2012)

Temperature(K)	E_{11}^{CNT} (TPa)	E_{22}^{CNT} (TPa)	G_{12}^{CNT} (TPa)	α_{11}^{CNT} ($10^{-6} / K$)	α_{22}^{CNT} ($10^{-6} / K$)
300	5.6466	7.0800	1.9445	3.4584	5.1682
400	5.5308	6.9348	1.9643	4.5361	5.0189
500	5.4744	6.8641	1.9644	4.6677	4.8943

Table 3 Mechanical properties of SWBNNTs (5,5) with $\nu=0.34$ (Ghorbanpour Arani *et al.* (2012), Mohammadimehr *et al.* 2016b)

$E_{11}^{BNNT} = E_{22}^{BNNT}$ (TPa)	G_{12}^{BNNT} (TPa)	α_{11}^{BNNT} ($10^{-6} / K$)	α_{22}^{BNNT} ($10^{-6} / K$)	η^{BNNT} ($10^{-6} F / m$)
1.799	0.6720	0.600	1.200	1.106

h_c that the material properties of these cores are showed that in Table 1 with details (Chakrabarti *et al.* 2007). It is noted that these cores generally do not use in common applications because they have large density and should not use as a core material. Thus, in the present study the effect of foam core is considered with $E_c=10 \text{ Mpa}$, $\nu_c=0.3$, $\rho_c=40 \text{ Kg/m}^3$ and $\alpha_c=1.8 \times 10^{-7}(1/K)$ (Zhao *et al.* 2017).

Moreover, the micro structure face sheets are chosen as smart composite materials with thickness h_b and h_t that they are reinforced by various nanotubes. In the other hand, in this work, the face sheets are made of composite material consist of a matrix and reinforcements that the upper and lower microplates reinforced by CNTs and BNNTs, respectively. The CNTs and BNNTs material properties are defined in Tables 2 and 3 (Ghorbanpour Arani *et al.* 2012, Mohammadimehr *et al.* 2016b, Mohammadimehr *et al.* 2016c, Zhu *et al.* 2012), respectively.

In Table 2, the material properties of CNTs are considered temperature-dependent and the relation between this properties and temperature are described in Eq. (1) as the

following form (Mohammadimehr and Mehrabi 2017)

$$\begin{cases} E_{11}^{CNT} = (7.425 \times 10^5 T^2) - (1.173 \times 10^9 T) + (5.9317 \times 10^{12}) \\ E_{22}^{CNT} = (9.3125 \times 10^5 T^2) - (1.471 \times 10^9 T) + (7.4375 \times 10^{12}) \\ G_{12}^{CNT} = (-2.4625 \times 10^5 T^2) + (2.96 \times 10^8 T) + (1.8779 \times 10^{12}) \\ \alpha_{11}^{CNT} = (-1.1826 \times 10^{-11} T^2) + (1.4850 \times 10^{-8} T) + (6.7913 \times 10^{-8}) \\ \alpha_{22}^{CNT} = (3.0875 \times 10^{-13} T^2) - (9.9350 \times 10^{-10} T) + (5.4385 \times 10^{-6}) \end{cases} \quad (1)$$

Also, the temperature-dependent material properties of polymeric matrix (PmPV) can be written as follows (Mohammadimehr *et al.* 2016d)

$$\begin{cases} E_m = (3.51 - 0.0047T) \text{ GPa} \\ \alpha_m = 45(1 + 0.0005\Delta T) \times 10^{-6} / K \\ \rho_m = 1150 \text{ kg} / m^3 \\ \nu_m = 0.34 \end{cases} \quad (2)$$

Finally, in order to calculate the equivalent mechanical and thermal properties of face sheets the Mori-Tanaka approach applied to derive the equivalent properties as follows (Mohammadimehr *et al.* 2016d)

$$\begin{cases} E_{11} = \eta_1 V_{XNT} E_{11}^{XNT} + V_m E_m \\ \frac{\eta_2}{E_{22}} = \frac{V_{XNT}}{E_{22}^{XNT}} + \frac{V_m}{E_m} \\ \frac{\eta_3}{G_{12}} = \frac{V_{XNT}}{G_{12}^{XNT}} + \frac{V_m}{G_m} \\ \rho = V_{XNT} \rho_{XNT} + V_m \rho_m \\ \nu_{12} = V_{XNT} \nu_{12}^{XNT} + V_m \nu_m \\ \alpha_{11} = V_{XNT} \alpha_{11}^{XNT} + V_m \alpha^m \\ \alpha_{22} = V_{XNT} \alpha_{22}^{XNT} + V_m \alpha^m \end{cases} \quad XNT \rightarrow: \begin{cases} CNT \\ BNNT \end{cases} \quad (3)$$

where E_m , ρ_m , ν_m and α^m are the elasticity modulus, density, Poisson's ratio and expansion thermal coefficient for the matrix, respectively that they are defined in Eq. (2). Also, E_{11}^{CNT} , E_{11}^{BNNT} , E_{22}^{CNT} , E_{22}^{BNNT} , G_{12}^{CNT} , G_{12}^{BNNT} , ν_{12}^{CNT} , ν_{12}^{BNNT} , α_{11}^{CNT} and α_{11}^{BNNT} introduce Young's modulus in various directions, shear modulus, Poisson's ratio and thermal expansion coefficient for the CNTs and BNNTs, respectively.

Moreover, V_m , V_{CNT} and V_{BNNT} are the volume fractions of matrix, carbon nanotubes and boron nitride nanotubes, respectively that there is linear relation between them as the following form (Ghorbanpour Arani *et al.* 2012)

$$\begin{cases} V_m + V_{CNT} = 1 \\ V_m + V_{BNNT} = 1 \end{cases} \quad (4)$$

In the Eq. (3), η_1 , η_2 and η_3 are the transformation forces between matrix and reinforcement that the values of them are depicted in Table 4.

3. Formulation

In the present study, in order to mathematical simulation of double-bonded micro composite sandwich plates

Table 4 Transformation forces between matrix and nanotubes (Mohammadimehr *et al.* 2016d)

Nanotubes volume Fractions	η_1	η_2	η_3
0.11	0.149	0.934	0.934
0.14	0.150	0.941	0.941
0.17	0.149	1.381	1.381

Table 5 γ_1 and γ_2 coefficients for the upper and lower micro sandwich SSDT plates

	γ_1 coefficient	γ_2 coefficient
Upper micro sandwich plate	0	1
Lower micro sandwich plate	1	0

reinforced by CNTs and BNNTs, the higher-order sinusoidal shear deformation plate theory (SSDT) is used based on the equivalent single layer sandwich (ESL) and MSGGT theories. Thus, at first, the displacement field equations are defined and then the Hamilton's principle and energy method are applied to make the governing equations of motions. Moreover, the relation between strain potential, displacement field, kinematic energy and external forces equations can be considered as follows:

3.1 Displacement field and strain-displacement equations

According to the SSDT, equations of displacement fields of double-bonded micro composites ESL sandwich plates reinforced by CNTs and BNNTs are defined as the following form (Kolahchi *et al.* 2017)

$$\begin{cases} u_j^{(i)}(x, y, z, t) = u_j^{(i)}(x, y, t) - z \frac{\partial w_{0j}^{(i)}(x, y, t)}{\partial x} + \Phi(z) \theta_j^{(i)}(x, y, t) \\ v_j^{(i)}(x, y, z, t) = v_j^{(i)}(x, y, t) - z \frac{\partial w_{0j}^{(i)}(x, y, t)}{\partial y} + \Phi(z) \theta_j^{(i)}(x, y, t) \\ w_j^{(i)}(x, y, z, t) = w_{0j}^{(i)}(x, y, t) \end{cases} \quad \left(\begin{array}{l} \Phi(z) = \frac{h}{\pi} \sin\left(\frac{\pi z}{h}\right) \\ j = t, c, b \\ i = 1, 2 \end{array} \right) \quad (5)$$

where $u_0^{(i)}$, $v_0^{(i)}$, $w_0^{(i)}$, $\theta_x^{(i)}$ and $\theta_y^{(i)}$ introduce the displacement components and angle of relation of cross-section of any point of the middle surface of the micro composite plate in the length, width and thickness directions, respectively. Also, i and j refer to the upper and lower double-bonded micro composite sandwich SSDT plates and top face sheet, core and bottom face sheet of each microplate, respectively. Moreover, with defining the displacement equations, the relations between strain and displacement in various micro plate directions can be described as follows

$$\begin{cases} \epsilon_{xx} = \frac{\partial u_x^{(i)}}{\partial x} = \frac{\partial u_x^{(i)}}{\partial x} - z \frac{\partial^2 w_{0x}^{(i)}}{\partial x^2} + \Phi(z) \frac{\partial \theta_x^{(i)}}{\partial x} \\ \epsilon_{yy} = \frac{\partial v_y^{(i)}}{\partial y} = \frac{\partial v_y^{(i)}}{\partial y} - z \frac{\partial^2 w_{0y}^{(i)}}{\partial y^2} + \Phi(z) \frac{\partial \theta_y^{(i)}}{\partial y} \\ \epsilon_{zz} = \frac{\partial w_z^{(i)}}{\partial z} = 0 \\ \epsilon_{xy} = \frac{1}{2} \left(\frac{\partial u_y^{(i)}}{\partial x} + \frac{\partial v_x^{(i)}}{\partial y} \right) = \frac{1}{2} \left(\frac{\partial u_y^{(i)}}{\partial x} + \frac{\partial v_x^{(i)}}{\partial y} + \Phi(z) \left(\frac{\partial \theta_y^{(i)}}{\partial x} + \frac{\partial \theta_x^{(i)}}{\partial y} \right) \right) - 2z \frac{\partial^2 w_{0xy}^{(i)}}{\partial x \partial y} \\ \epsilon_{xz} = \frac{1}{2} \left(\frac{\partial u_x^{(i)}}{\partial z} + \frac{\partial w_z^{(i)}}{\partial x} \right) = \frac{1}{2} \frac{\partial \Phi(z)}{\partial z} \theta_x^{(i)} \\ \epsilon_{yz} = \frac{1}{2} \left(\frac{\partial v_y^{(i)}}{\partial z} + \frac{\partial w_z^{(i)}}{\partial y} \right) = \frac{1}{2} \frac{\partial \Phi(z)}{\partial z} \theta_y^{(i)} \end{cases} \quad \left(\begin{array}{l} \Phi(z) = \frac{h}{\pi} \sin\left(\frac{\pi z}{h}\right) \\ j = t, c, b \\ i = 1, 2 \end{array} \right) \quad (6)$$

3.2 Strain potential energy

One of the newest non-classical theories in the micro and nano scale is the most general strain gradient theory (MSGGT) that it is consist of strain classic and third order strain gradient tensors, stress classic vector and higher order stresses tensor. It is noted that MSGGT embrace the other

micro/nano theories such as CT, MCST and MSGT. Also, this theory by considering the effects of magnetic and electric fields that they are defined because of the presence of carbon and boron nitride nanotubes can be written as the following form (Shooshtari and Razavi 2015)

$$U = \frac{1}{2} \int_V (\sigma_{ij} \epsilon_{ij} + \tau_{ijk} \xi_{ijk} - D_i E_i - B_i H_i) dV \quad (7)$$

By applying the variation method into the Eq. (7) the first variation of strain potential energy is described as follows

$$\delta U = \int_V (\sigma_{ij} \delta \epsilon_{ij} + \tau_{ijk} \delta \xi_{ijk} - \gamma_1 D_i \delta E_i - \gamma_2 B_i \delta H_i) dV \quad (8)$$

In the above equation, γ_1 and γ_2 are the coefficients of the electric and magnetic fields, respectively that according to Table 5 they are equal to 0 and 1 for each upper and lower micro sandwich plates.

where ϵ_{ij} , ξ_{ijk} , σ_{ij} , τ_{ijk} , D_i , B_i , E_i and H_i are the strain tensor, higher order strain gradient tensor, classical stress component, higher order stresses tensor, electric and magnetic displacements and electric and magnetic fields, respectively. These components are introduced into the Eqs. (5) to (18) as follows (Akbari Alashti and Khorsand 2012, Ansari *et al.* 2015, Ansari *et al.* 2013, Nasihatgozar *et al.* 2016)

$$\epsilon_{ij} = \frac{1}{2} \left(\frac{\partial u_i}{\partial x_j} + \frac{\partial u_j}{\partial x_i} \right) \quad (9)$$

$$\sigma_{ij} = Q_{ij} \epsilon_{ij} \quad (10)$$

$$\xi_{ijk} = \xi_{ikj} = \epsilon_{jk,i} = \frac{1}{2} (u_{j,k} + u_{k,j})_{,i} \quad (11)$$

$$\tau_{ijk} = \frac{1}{2} a_i (\xi_{ipq} \delta_{qj} + 2\xi_{ppq} \delta_{jk} + \xi_{ppq} \delta_{ik}) + 2a_1 \xi_{ppq} \delta_{jk} + a_3 (\xi_{ppk} \delta_{ij} + \xi_{ppk} \delta_{ik}) + 2a_4 \xi_{ijk} + a_5 (\xi_{ji} + \xi_{ij}) \quad (12)$$

where u_i , G and δ are the displacement components in x , y and z -directions, shear modulus and Kronecker delta, respectively. Also, a_1 , a_2 , a_3 , a_4 and a_5 are the additional material length scale parameters and l_0 , l_1 and l_2 are the material length scale parameters that they are different for the micro/nano scale systems.

• Higher order strain gradient components

$$\begin{cases} \epsilon_{xx}^{(i)} = \frac{\partial^2 u_x^{(i)}}{\partial x^2} = \frac{\partial^2 u_x^{(i)}}{\partial x^2} - z \frac{\partial^3 w_{0x}^{(i)}}{\partial x^3} + \Phi(z) \frac{\partial^2 \theta_x^{(i)}}{\partial x^2} \\ \epsilon_{yy}^{(i)} = \frac{1}{2} \left(\frac{\partial^2 u_y^{(i)}}{\partial x \partial y} + \frac{\partial^2 v_x^{(i)}}{\partial x \partial y} \right) = \frac{1}{2} \left(\frac{\partial^2 u_y^{(i)}}{\partial x \partial y} + \frac{\partial^2 v_x^{(i)}}{\partial x \partial y} + \Phi(z) \left(\frac{\partial^2 \theta_y^{(i)}}{\partial x \partial y} + \frac{\partial^2 \theta_x^{(i)}}{\partial x \partial y} \right) \right) - 2z \frac{\partial^3 w_{0xy}^{(i)}}{\partial x \partial y} \\ \epsilon_{xz}^{(i)} = \frac{1}{2} \left(\frac{\partial^2 u_x^{(i)}}{\partial x \partial z} + \frac{\partial^2 w_z^{(i)}}{\partial x \partial z} \right) = \frac{1}{2} \frac{\partial \Phi(z)}{\partial z} \frac{\partial \theta_x^{(i)}}{\partial x} \\ \epsilon_{yz}^{(i)} = \frac{1}{2} \left(\frac{\partial^2 v_y^{(i)}}{\partial y \partial z} + \frac{\partial^2 w_z^{(i)}}{\partial y \partial z} \right) = \frac{1}{2} \frac{\partial \Phi(z)}{\partial z} \frac{\partial \theta_y^{(i)}}{\partial y} \\ \epsilon_{zz}^{(i)} = \frac{\partial^2 w_z^{(i)}}{\partial z^2} = 0 \end{cases} \quad \left(\begin{array}{l} \Phi(z) = \frac{h}{\pi} \sin\left(\frac{\pi z}{h}\right) \\ i = 1, 2 \end{array} \right) \quad (13a)$$

$$\left\{ \begin{aligned} \epsilon_{xx}^{(i)} &= \frac{\partial^2 u^{(i)}}{\partial x^2} = \frac{\partial^2 w^{(i)}}{\partial x^2} - z \frac{\partial^2 w^{(i)}}{\partial x^2} + \Phi(z) \frac{\partial^2 \theta^{(i)}}{\partial x^2} \\ \epsilon_{yy}^{(i)} &= \frac{1}{2} \left(\frac{\partial^2 u^{(i)}}{\partial y^2} + \frac{\partial^2 v^{(i)}}{\partial x^2} \right) = \frac{1}{2} \left(\frac{\partial^2 u_0^{(i)}}{\partial y^2} - 2z \frac{\partial^2 w_0^{(i)}}{\partial x^2} + \Phi(z) \frac{\partial^2 \theta^{(i)}}{\partial y^2} + \frac{\partial^2 v_0^{(i)}}{\partial x^2} + \Phi(z) \frac{\partial^2 \theta^{(i)}}{\partial x^2} \right) \\ \epsilon_{zz}^{(i)} &= \frac{1}{2} \left(\frac{\partial^2 u^{(i)}}{\partial z^2} + \frac{\partial^2 w^{(i)}}{\partial x^2} \right) = \frac{1}{2} \left[\frac{\partial \Phi(z)}{\partial z} \frac{\partial \theta^{(i)}}{\partial y} \right] \\ \epsilon_{xy}^{(i)} &= \frac{\partial^2 v^{(i)}}{\partial y^2} = \frac{\partial^2 v_0^{(i)}}{\partial y^2} - z \frac{\partial^2 w_0^{(i)}}{\partial y^2} + \Phi(z) \frac{\partial^2 \theta^{(i)}}{\partial y^2} \\ \epsilon_{yz}^{(i)} &= \frac{1}{2} \left(\frac{\partial^2 v^{(i)}}{\partial z^2} + \frac{\partial^2 w^{(i)}}{\partial y^2} \right) = \frac{1}{2} \left[\frac{\partial \Phi(z)}{\partial z} \frac{\partial \theta^{(i)}}{\partial y} \right] \\ \epsilon_{zx}^{(i)} &= \frac{\partial^2 w^{(i)}}{\partial z^2} = 0 \end{aligned} \right. \quad \left(\Phi(z) = \frac{h}{\pi} \sin\left(\frac{\pi z}{h}\right) \right) \quad (13b)$$

$$\left\{ \begin{aligned} \epsilon_{xx}^{(i)} &= \frac{\partial^2 u^{(i)}}{\partial x^2} = \frac{\partial^2 w^{(i)}}{\partial x^2} + \frac{\partial \Phi(z)}{\partial z} \frac{\partial \theta^{(i)}}{\partial x} \\ \epsilon_{yy}^{(i)} &= \frac{1}{2} \left(\frac{\partial^2 u^{(i)}}{\partial y^2} + \frac{\partial^2 v^{(i)}}{\partial x^2} \right) = \frac{1}{2} \left[\frac{\partial \Phi(z)}{\partial z} \left(\frac{\partial \theta^{(i)}}{\partial y} + \frac{\partial \theta^{(i)}}{\partial x} \right) - 2 \frac{\partial^2 w_0^{(i)}}{\partial x^2} \right] \\ \epsilon_{zz}^{(i)} &= \frac{1}{2} \left(\frac{\partial^2 u^{(i)}}{\partial z^2} + \frac{\partial^2 w^{(i)}}{\partial x^2} \right) = \frac{1}{2} \frac{\partial^2 \Phi(z)}{\partial z^2} \theta^{(i)} \\ \epsilon_{xy}^{(i)} &= \frac{\partial^2 v^{(i)}}{\partial z^2} = \frac{\partial^2 w^{(i)}}{\partial y^2} + \frac{\partial \Phi(z)}{\partial z} \frac{\partial \theta^{(i)}}{\partial y} \\ \epsilon_{yz}^{(i)} &= \frac{1}{2} \left(\frac{\partial^2 v^{(i)}}{\partial z^2} + \frac{\partial^2 w^{(i)}}{\partial y^2} \right) = \frac{1}{2} \frac{\partial^2 \Phi(z)}{\partial z^2} \theta^{(i)} \\ \epsilon_{zx}^{(i)} &= \frac{\partial^2 w^{(i)}}{\partial z^2} = 0 \end{aligned} \right. \quad \left(\Phi(z) = \frac{h}{\pi} \sin\left(\frac{\pi z}{h}\right) \right) \quad (13c)$$

• Classical stress components (Mohammadimehr *et al.* 2016d)

$$\left\{ \begin{aligned} \sigma_x \\ \sigma_y \\ \sigma_z \\ \tau_{yz} \\ \tau_{xz} \\ \tau_{xy} \end{aligned} \right\} = \left[\begin{aligned} Q_{11} & Q_{12} & Q_{13} & 0 & 0 & 0 \\ Q_{12} & Q_{22} & Q_{23} & 0 & 0 & 0 \\ Q_{13} & Q_{23} & Q_{33} & 0 & 0 & 0 \\ 0 & 0 & 0 & Q_{44} & 0 & 0 \\ 0 & 0 & 0 & 0 & Q_{55} & 0 \\ 0 & 0 & 0 & 0 & 0 & Q_{66} \end{aligned} \right] \left\{ \begin{aligned} \epsilon_x - \alpha_{11} \Delta T \\ \epsilon_y - \alpha_{22} \Delta T \\ \epsilon_z \\ \gamma_{yz} \\ \gamma_{xz} \\ \gamma_{xy} \end{aligned} \right\} \quad (14)$$

where Q is the stiffness matrix reinforced by nanotubes that the components of this matrix can be described as follows (Zhu *et al.* 2012)

$$Q_{11} = \frac{E_{11}}{1 - \nu_{12}\nu_{21}}; Q_{22} = \frac{E_{22}}{1 - \nu_{12}\nu_{21}}; Q_{12} = \frac{\nu_{21}E_{11}}{1 - \nu_{12}\nu_{21}}; Q_{44} = G_{23}; Q_{55} = G_{13}; Q_{66} = G_{12} \quad (15)$$

Also, α_{11} , α_{22} and ΔT are the thermal expansion coefficients in the length and width plate directions and temperature changes, respectively.

• Components of higher order stresses tensor (Zhu *et al.* 2012, Ansari *et al.* 2015)

$$\left\{ \begin{aligned} \epsilon_{xx}^{(i)} &= a_1(2\epsilon_{xx}^{(i)} + \epsilon_{yy}^{(i)} + \epsilon_{zz}^{(i)} + \epsilon_{xx}^{(i)} + \epsilon_{yy}^{(i)} + \epsilon_{zz}^{(i)}) + 2a_2(\epsilon_{xx}^{(i)} + \epsilon_{yy}^{(i)} + \epsilon_{zz}^{(i)}) \\ &+ a_3(2\epsilon_{xx}^{(i)} + 2\epsilon_{yy}^{(i)} + 2\epsilon_{zz}^{(i)}) + 2a_4\epsilon_{xx}^{(i)} + 2a_5\epsilon_{xx}^{(i)} \\ \epsilon_{xx}^{(i)} &= \frac{a_1}{2}(\epsilon_{xx}^{(i)} + \epsilon_{yy}^{(i)} + \epsilon_{zz}^{(i)}) + a_3(\epsilon_{xx}^{(i)} + \epsilon_{yy}^{(i)} + \epsilon_{zz}^{(i)}) + 2a_4\epsilon_{xx}^{(i)} + a_5(\epsilon_{xx}^{(i)} + \epsilon_{yy}^{(i)}) \\ \epsilon_{yy}^{(i)} &= \frac{a_1}{2}(\epsilon_{xx}^{(i)} + \epsilon_{yy}^{(i)} + \epsilon_{zz}^{(i)}) + a_3(\epsilon_{xx}^{(i)} + \epsilon_{yy}^{(i)} + \epsilon_{zz}^{(i)}) + 2a_4\epsilon_{yy}^{(i)} + a_5(\epsilon_{xx}^{(i)} + \epsilon_{yy}^{(i)}) \\ \epsilon_{zz}^{(i)} &= 2a_4\epsilon_{zz}^{(i)} + a_5(\epsilon_{xx}^{(i)} + \epsilon_{yy}^{(i)}) \\ \epsilon_{zz}^{(i)} &= a_4(\epsilon_{xx}^{(i)} + \epsilon_{yy}^{(i)} + \epsilon_{zz}^{(i)}) + 2a_2(\epsilon_{xx}^{(i)} + \epsilon_{yy}^{(i)} + \epsilon_{zz}^{(i)}) + 2a_4\epsilon_{zz}^{(i)} + 2a_5\epsilon_{zz}^{(i)} \end{aligned} \right. \quad (i=1,2) \quad (16a)$$

$$\left\{ \begin{aligned} \tau_{xx}^{(i)} &= a_1(\epsilon_{xx}^{(i)} + \epsilon_{yy}^{(i)} + \epsilon_{zz}^{(i)}) + 2a_2(\epsilon_{xx}^{(i)} + \epsilon_{yy}^{(i)} + \epsilon_{zz}^{(i)}) + 2a_4\epsilon_{xx}^{(i)} + 2a_5\epsilon_{xx}^{(i)} \\ \tau_{yy}^{(i)} &= \frac{a_1}{2}(\epsilon_{xx}^{(i)} + \epsilon_{yy}^{(i)} + \epsilon_{zz}^{(i)}) + a_3(\epsilon_{xx}^{(i)} + \epsilon_{yy}^{(i)} + \epsilon_{zz}^{(i)}) + 2a_4\epsilon_{yy}^{(i)} + a_5(\epsilon_{xx}^{(i)} + \epsilon_{yy}^{(i)}) \\ &+ 2a_3(\epsilon_{xx}^{(i)} + \epsilon_{yy}^{(i)} + \epsilon_{zz}^{(i)}) + 2a_4\epsilon_{yy}^{(i)} + 2a_5\epsilon_{yy}^{(i)} \\ \tau_{yz}^{(i)} &= \frac{a_1}{2}(\epsilon_{xx}^{(i)} + \epsilon_{yy}^{(i)} + \epsilon_{zz}^{(i)}) + a_3(\epsilon_{xx}^{(i)} + \epsilon_{yy}^{(i)} + \epsilon_{zz}^{(i)}) + 2a_4\epsilon_{yz}^{(i)} + a_5(\epsilon_{xx}^{(i)} + \epsilon_{yy}^{(i)}) \\ \tau_{xz}^{(i)} &= a_4(\epsilon_{xx}^{(i)} + \epsilon_{yy}^{(i)} + \epsilon_{zz}^{(i)}) + 2a_2(\epsilon_{xx}^{(i)} + \epsilon_{yy}^{(i)} + \epsilon_{zz}^{(i)}) + 2a_4\epsilon_{xz}^{(i)} + 2a_5\epsilon_{xz}^{(i)} \end{aligned} \right. \quad (i=1,2) \quad (16b)$$

$$\left\{ \begin{aligned} \tau_{xx}^{(i)} &= a_1(\epsilon_{xx}^{(i)} + \epsilon_{yy}^{(i)} + \epsilon_{zz}^{(i)}) + 2a_2(\epsilon_{xx}^{(i)} + \epsilon_{yy}^{(i)} + \epsilon_{zz}^{(i)}) + 2a_4\epsilon_{xx}^{(i)} + 2a_5\epsilon_{xx}^{(i)} \\ \tau_{yy}^{(i)} &= 2a_4\epsilon_{yy}^{(i)} + a_5(\epsilon_{xx}^{(i)} + \epsilon_{yy}^{(i)}) \\ \tau_{zz}^{(i)} &= \frac{a_1}{2}(\epsilon_{xx}^{(i)} + \epsilon_{yy}^{(i)} + \epsilon_{zz}^{(i)}) + a_3(\epsilon_{xx}^{(i)} + \epsilon_{yy}^{(i)} + \epsilon_{zz}^{(i)}) + 2a_4\epsilon_{zz}^{(i)} + a_5(\epsilon_{xx}^{(i)} + \epsilon_{yy}^{(i)}) \\ \tau_{xy}^{(i)} &= a_1(\epsilon_{xx}^{(i)} + \epsilon_{yy}^{(i)} + \epsilon_{zz}^{(i)}) + 2a_2(\epsilon_{xx}^{(i)} + \epsilon_{yy}^{(i)} + \epsilon_{zz}^{(i)}) + 2a_4\epsilon_{xy}^{(i)} + 2a_5\epsilon_{xy}^{(i)} \\ \tau_{yz}^{(i)} &= \frac{a_1}{2}(\epsilon_{xx}^{(i)} + \epsilon_{yy}^{(i)} + \epsilon_{zz}^{(i)}) + a_3(\epsilon_{xx}^{(i)} + \epsilon_{yy}^{(i)} + \epsilon_{zz}^{(i)}) + 2a_4\epsilon_{yz}^{(i)} + a_5(\epsilon_{xx}^{(i)} + \epsilon_{yy}^{(i)}) \\ \tau_{zx}^{(i)} &= a_4(\epsilon_{xx}^{(i)} + \epsilon_{yy}^{(i)} + \epsilon_{zz}^{(i)}) + 2\epsilon_{zz}^{(i)} + \epsilon_{xx}^{(i)} + \epsilon_{yy}^{(i)} + 2a_2(\epsilon_{xx}^{(i)} + \epsilon_{yy}^{(i)} + \epsilon_{zz}^{(i)}) \\ &+ 2a_3(\epsilon_{xx}^{(i)} + \epsilon_{yy}^{(i)} + \epsilon_{zz}^{(i)}) + 2a_4\epsilon_{zx}^{(i)} + 2a_5\epsilon_{zx}^{(i)} \end{aligned} \right. \quad (i=1,2) \quad (16c)$$

• Electric and magnetic fields components

$$\left\{ \begin{aligned} D_x &= \lambda_1 E_x + p_1 \Delta T \\ E_x &= -\frac{\partial \varphi_E(x, z, t)}{\partial x} \\ \varphi_E &= -\cos\left(\frac{\pi z}{h}\right) \varphi_E(x, t) \end{aligned} \right. \quad (17)$$

$$\left\{ \begin{aligned} B_i &= \mu_i H_i + \eta_i \Delta T \\ H_i &= -\frac{\partial \varphi_H(x, y, z, t)}{\partial x_i} \\ \varphi_H &= -\cos\left(\frac{\pi z}{h}\right) \varphi_H(x, y, t) \end{aligned} \right. \quad (i=1,2) \quad (18)$$

where, λ_1 , p_x , $\varphi_E(x, z, t)$, μ_i , η_i and $\varphi_H(x, y, z, t)$ are the dielectric constant, pyro-electric constant, electrical potential in x -direction, magnetic constant, pyro-magnetic constant and magnetic potential in x and y -directions, respectively.

The first variations of strain potential energy based on MGS GT can be obtained by substituting Eq. (6) and Eqs. (9)-(18) into the Eq. (8)

$$\delta U = \int_0^b \int_0^a \left\{ \begin{aligned} &[-N_{xx,x}^i - N_{yy,y}^i + T_{xxx,xxx}^{(0i)} + T_{xxx,yy}^{(0i)} + T_{xxx,yy}^{(0i)} + T_{xxx,yy}^{(0i)}] \delta u_0^{(i)} \\ &+ [-N_{yy,y}^i - N_{xx,x}^i + T_{xxx,xxx}^{(0i)} + T_{xxx,yy}^{(0i)} + T_{xxx,yy}^{(0i)} + T_{xxx,yy}^{(0i)}] \delta v_0^{(i)} \\ &+ [-M_{xx,xx}^i - 2M_{yy,yy}^i - M_{zz,zz}^i + T_{xxx,xxx}^{(1i)} + T_{xxx,yy}^{(1i)} + 2T_{xxx,yy}^{(1i)} + T_{xxx,yy}^{(1i)} \\ &+ T_{xxx,yy}^{(1i)} + 2T_{xxx,yy}^{(1i)} + T_{xxx,yy}^{(1i)} + T_{xxx,yy}^{(1i)} - 2T_{xxx,yy}^{(1i)} - T_{xxx,yy}^{(1i)}] \delta w_0^{(i)} \\ &+ [T_{xxx,xx}^{(Ri)} + T_{xxx,yy}^{(Ri)} - T_{xxx,xx}^{(Ri)} + T_{xxx,yy}^{(Ri)} + T_{xxx,yy}^{(Ri)} - T_{xxx,yy}^{(Ri)} - T_{xxx,yy}^{(Ri)}] \delta \theta_x^{(i)} \\ &+ [-T_{xxx,yy}^{(Ri)} + T_{xxx,xx}^{(Ri)} - R_{xx,xx}^i - R_{yy,yy}^i + R_{zz,zz}^i] \delta \theta_y^{(i)} \\ &+ [T_{xxx,xx}^{(Ri)} + T_{xxx,yy}^{(Ri)} - T_{xxx,xx}^{(Ri)} + T_{xxx,yy}^{(Ri)} + T_{xxx,yy}^{(Ri)} - T_{xxx,yy}^{(Ri)} - T_{xxx,yy}^{(Ri)}] \delta \theta_z^{(i)} \\ &+ [-T_{xxx,yy}^{(Ri)} + T_{xxx,xx}^{(Ri)} - R_{xx,xx}^i - R_{yy,yy}^i + R_{zz,zz}^i] \delta \theta_x^{(i)} \\ &+ [B_x^{(Rp)} + B_y^{(Rp)}] \delta \varphi_H + [D_x^{(Rp)}] \delta \varphi_E \end{aligned} \right\} dx dy \quad (19)$$

where

$$(N_{xx}^i, N_{yy}^i, N_{xy}^i) = \int_{\frac{h}{2}}^{\frac{h}{2}} (\sigma_x^i, \sigma_y^i, \tau_{xy}^i) dz + \int_{\frac{h}{2}}^{\frac{h}{2}} (\sigma_x^i, \sigma_y^i, \tau_{xy}^i) dz + \int_{\frac{h}{2}}^{\frac{h}{2}} (\sigma_x^i, \sigma_y^i, \tau_{xy}^i) dz \quad (20a)$$

$$(M_{xx}^i, M_{yy}^i, M_{zz}^i) = \int_{\frac{h}{2}}^{\frac{h}{2}} (\sigma_x^i, \sigma_y^i, \tau_{xy}^i) z dz + \int_{\frac{h}{2}}^{\frac{h}{2}} (\sigma_x^i, \sigma_y^i, \tau_{xy}^i) z dz + \int_{\frac{h}{2}}^{\frac{h}{2}} (\sigma_x^i, \sigma_y^i, \tau_{xy}^i) z dz \quad (20b)$$

$$(R_{xx}^i, R_{yy}^i, R_{zz}^i) = \int_{\frac{h}{2}}^{\frac{h}{2}} (\sigma_x^i, \sigma_y^i, \tau_{xy}^i) \Phi(z) dz + \int_{\frac{h}{2}}^{\frac{h}{2}} (\sigma_x^i, \sigma_y^i, \tau_{xy}^i) \Phi(z) dz + \int_{\frac{h}{2}}^{\frac{h}{2}} (\sigma_x^i, \sigma_y^i, \tau_{xy}^i) \Phi(z) dz \quad (20c)$$

$$(R_{xz}^{(P)}, R_{yz}^{(P)}) = \int_{\frac{h}{2}}^{\frac{h}{2} + \frac{h_0}{2}} (\tau_{xz}^i, \tau_{yz}^i) \frac{\partial \Phi(z)}{\partial z} dz + \int_{\frac{h}{2}}^{\frac{h}{2} - \frac{h_0}{2}} (\tau_{xz}^i, \tau_{yz}^i) \frac{\partial \Phi(z)}{\partial z} dz + \int_{\frac{h}{2} - \frac{h_0}{2}}^{\frac{h}{2}} (\tau_{xz}^i, \tau_{yz}^i) \frac{\partial \Phi(z)}{\partial z} dz \quad (20d)$$

$$(T_{xx}^{(0)}, T_{xy}^{(0)}, T_{xx}^{(0)}, T_{yy}^{(0)}, T_{xx}^{(0)}, T_{yy}^{(0)}, T_{xx}^{(0)}, T_{yy}^{(0)}) = \int_{\frac{h}{2}}^{\frac{h}{2} + \frac{h_0}{2}} (\tau_{xx}^i, \tau_{xy}^i, \tau_{xx}^i, \tau_{yy}^i, \tau_{xx}^i, \tau_{yy}^i, \tau_{xx}^i, \tau_{yy}^i) dz + \int_{\frac{h}{2}}^{\frac{h}{2} - \frac{h_0}{2}} (\tau_{xx}^i, \tau_{xy}^i, \tau_{xx}^i, \tau_{yy}^i, \tau_{xx}^i, \tau_{yy}^i, \tau_{xx}^i, \tau_{yy}^i) dz + \int_{\frac{h}{2} - \frac{h_0}{2}}^{\frac{h}{2}} (\tau_{xx}^i, \tau_{xy}^i, \tau_{xx}^i, \tau_{yy}^i, \tau_{xx}^i, \tau_{yy}^i, \tau_{xx}^i, \tau_{yy}^i) dz \quad (21a)$$

$$(T_{xx}^{(1)}, T_{xy}^{(1)}, T_{xx}^{(1)}, T_{yy}^{(1)}, T_{xx}^{(1)}, T_{yy}^{(1)}) = \int_{\frac{h}{2}}^{\frac{h}{2} + \frac{h_0}{2}} (\tau_{xx}^i, \tau_{xy}^i, \tau_{xx}^i, \tau_{yy}^i, \tau_{xx}^i, \tau_{yy}^i) z dz + \int_{\frac{h}{2}}^{\frac{h}{2} - \frac{h_0}{2}} (\tau_{xx}^i, \tau_{xy}^i, \tau_{xx}^i, \tau_{yy}^i, \tau_{xx}^i, \tau_{yy}^i) z dz + \int_{\frac{h}{2} - \frac{h_0}{2}}^{\frac{h}{2}} (\tau_{xx}^i, \tau_{xy}^i, \tau_{xx}^i, \tau_{yy}^i, \tau_{xx}^i, \tau_{yy}^i) z dz \quad (21b)$$

$$(T_{xx}^{(R)}, T_{xy}^{(R)}, T_{xx}^{(R)}, T_{yy}^{(R)}, T_{xx}^{(R)}, T_{yy}^{(R)}) = \int_{\frac{h}{2}}^{\frac{h}{2} + \frac{h_0}{2}} (\tau_{xx}^i, \tau_{xy}^i, \tau_{xx}^i, \tau_{yy}^i, \tau_{xx}^i, \tau_{yy}^i) \Phi(z) dz + \int_{\frac{h}{2}}^{\frac{h}{2} - \frac{h_0}{2}} (\tau_{xx}^i, \tau_{xy}^i, \tau_{xx}^i, \tau_{yy}^i, \tau_{xx}^i, \tau_{yy}^i) \Phi(z) dz + \int_{\frac{h}{2} - \frac{h_0}{2}}^{\frac{h}{2}} (\tau_{xx}^i, \tau_{xy}^i, \tau_{xx}^i, \tau_{yy}^i, \tau_{xx}^i, \tau_{yy}^i) \Phi(z) dz \quad (21c)$$

$$(T_{xx}^{(R_p)}, T_{xy}^{(R_p)}, T_{xx}^{(R_p)}, T_{yy}^{(R_p)}, T_{xx}^{(R_p)}, T_{yy}^{(R_p)}) = \int_{\frac{h}{2}}^{\frac{h}{2} + \frac{h_0}{2}} (\tau_{xx}^i, \tau_{xy}^i, \tau_{xx}^i, \tau_{yy}^i, \tau_{xx}^i, \tau_{yy}^i) \frac{\partial \Phi(z)}{\partial z} dz + \int_{\frac{h}{2}}^{\frac{h}{2} - \frac{h_0}{2}} (\tau_{xx}^i, \tau_{xy}^i, \tau_{xx}^i, \tau_{yy}^i, \tau_{xx}^i, \tau_{yy}^i) \frac{\partial \Phi(z)}{\partial z} dz + \int_{\frac{h}{2} - \frac{h_0}{2}}^{\frac{h}{2}} (\tau_{xx}^i, \tau_{xy}^i, \tau_{xx}^i, \tau_{yy}^i, \tau_{xx}^i, \tau_{yy}^i) \frac{\partial \Phi(z)}{\partial z} dz \quad (21d)$$

$$(T_{xx}^{(R_p)}, T_{xx}^{(R_p)}) = \int_{\frac{h}{2}}^{\frac{h}{2} + \frac{h_0}{2}} (\tau_{xx}^i, \tau_{xx}^i) \frac{\partial^2 \Phi(z)}{\partial z^2} dz + \int_{\frac{h}{2}}^{\frac{h}{2} - \frac{h_0}{2}} (\tau_{xx}^i, \tau_{xx}^i) \frac{\partial^2 \Phi(z)}{\partial z^2} dz + \int_{\frac{h}{2} - \frac{h_0}{2}}^{\frac{h}{2}} (\tau_{xx}^i, \tau_{xx}^i) \frac{\partial^2 \Phi(z)}{\partial z^2} dz \quad (21e)$$

$$(B_x^{(R)}, B_y^{(R)}, D_x^{(R)}) = \int_{\frac{h}{2}}^{\frac{h}{2} + \frac{h_0}{2}} (B_{x,x}, B_{y,y}, D_{x,x}) \frac{\partial \Phi(z)}{\partial z} dz + \int_{\frac{h}{2}}^{\frac{h}{2} - \frac{h_0}{2}} (B_{x,x}, B_{y,y}, D_{x,x}) \frac{\partial \Phi(z)}{\partial z} dz \quad (22)$$

3.3 Kinetic energy

The kinetic energy equation of double-bonded micro sandwich composite plates reinforced by CNTs and BNNTs can be defined as follows (Ghorbanpour Arani *et al.* 2016)

$$T = T_{top}^1 + T_{cor}^1 + T_{bottom}^1 + T_{top}^2 + T_{cor}^2 + T_{bottom}^2$$

$$T = \frac{1}{2} \int_V \left\{ \begin{aligned} & \left[\rho_j^{(1)} \left(\frac{\partial w_j^{(1)}}{\partial t} \right)^2 + \left(\frac{\partial v_j^{(1)}}{\partial t} \right)^2 + \left(\frac{\partial w_j^{(1)}}{\partial t} \right)^2 \right] + \left[\rho_c^{(1)} \left(\frac{\partial w_c^{(1)}}{\partial t} \right)^2 + \left(\frac{\partial v_c^{(1)}}{\partial t} \right)^2 + \left(\frac{\partial w_c^{(1)}}{\partial t} \right)^2 \right] \\ & \left[\rho_b^{(1)} \left(\frac{\partial w_b^{(1)}}{\partial t} \right)^2 + \left(\frac{\partial v_b^{(1)}}{\partial t} \right)^2 + \left(\frac{\partial w_b^{(1)}}{\partial t} \right)^2 \right] \\ & \left[\rho_j^{(2)} \left(\frac{\partial w_j^{(2)}}{\partial t} \right)^2 + \left(\frac{\partial v_j^{(2)}}{\partial t} \right)^2 + \left(\frac{\partial w_j^{(2)}}{\partial t} \right)^2 \right] + \left[\rho_c^{(2)} \left(\frac{\partial w_c^{(2)}}{\partial t} \right)^2 + \left(\frac{\partial v_c^{(2)}}{\partial t} \right)^2 + \left(\frac{\partial w_c^{(2)}}{\partial t} \right)^2 \right] \\ & \left[\rho_b^{(2)} \left(\frac{\partial w_b^{(2)}}{\partial t} \right)^2 + \left(\frac{\partial v_b^{(2)}}{\partial t} \right)^2 + \left(\frac{\partial w_b^{(2)}}{\partial t} \right)^2 \right] \end{aligned} \right\} dV \quad (23)$$

$$T = \frac{1}{2} \int_V \left\{ \left[\rho_j^{(i)} \left(\frac{\partial w_j^{(i)}}{\partial t} \right)^2 + \left(\frac{\partial v_j^{(i)}}{\partial t} \right)^2 + \left(\frac{\partial w_j^{(i)}}{\partial t} \right)^2 \right] \right\} dV \quad \Rightarrow \quad \left(\begin{matrix} j = i, c, b \\ i = 1, 2 \end{matrix} \right)$$

where $T_{top}^{(1)}, T_{cor}^{(1)}, T_{bottom}^{(1)}, T_{top}^{(2)}, T_{cor}^{(2)}, T_{bottom}^{(2)}$ and $\rho_j^{(i)}$ refer to the kinetic energy of top face sheets, core, and bottom face sheets for the upper and lower microplates and density of each layers, respectively. Thus, Eq. (23) after applying the variation method rewritten as the following form

$$\delta T = \delta T_{top}^1 + \delta T_{cor}^1 + \delta T_{bottom}^1 + \delta T_{top}^2 + \delta T_{cor}^2 + \delta T_{bottom}^2$$

$$\delta T = \int_V \left\{ \left[\rho_j^{(i)} \left(\frac{\partial w_j^{(i)}}{\partial t} \right) \left(\frac{\partial \delta w_j^{(i)}}{\partial t} \right) + \left(\frac{\partial v_j^{(i)}}{\partial t} \right) \left(\frac{\partial \delta v_j^{(i)}}{\partial t} \right) + \left(\frac{\partial w_j^{(i)}}{\partial t} \right) \left(\frac{\partial \delta w_j^{(i)}}{\partial t} \right) \right] \right\} dV \quad (j = i, c, b) \quad (24)$$

Substituting Eq. (5) into the Eq. (24) and defining the inertia terms based on the Eq. (26) the first variation of kinetic energy of double-bonded sandwich micro composite SSDT plates reinforced by CNTs and BNNTs are calculated as follows

$$\delta T = - \int_A \left\{ \begin{aligned} & \left[I_0^i u_{0,x}^{(i)} - I_1^i w_{0,x}^{(i)} + R_1^i \theta_{x,x}^{(i)} \right] \delta w_0^{(i)} \\ & + \left[I_0^i v_{0,y}^{(i)} - I_1^i w_{0,y}^{(i)} + R_1^i \theta_{y,y}^{(i)} \right] \delta w_0^{(i)} \\ & + \left[I_1^i u_{0,x}^{(i)} - I_2^i w_{0,x}^{(i)} + IR_1^i \theta_{x,x}^{(i)} + I_1^i v_{0,y}^{(i)} \right] \delta w_0^{(i)} \\ & - \left[I_2^i w_{0,y}^{(i)} + IR_1^i \theta_{y,y}^{(i)} + I_0^i w_{0,x}^{(i)} \right] \delta w_0^{(i)} \\ & + \left[R_1^i u_{0,x}^{(i)} - IR_1^i w_{0,x}^{(i)} + R_2^i \theta_{x,x}^{(i)} \right] \delta \theta^{(i)} \\ & + \left[R_1^i v_{0,y}^{(i)} - IR_1^i w_{0,y}^{(i)} + R_2^i \theta_{y,y}^{(i)} \right] \delta \theta^{(i)} \end{aligned} \right\} dA \quad i = \{1, 2\} \quad (25)$$

where

$$(I_0^i, I_1^i, I_2^i, R_1^i, R_2^i, IR_1^i) = \int_{\frac{h}{2}}^{\frac{h}{2} + \frac{h_0}{2}} \rho_j^i (1, z, z^2, \Phi(z), \Phi^2(z), z \Phi(z)) dz + \int_{\frac{h}{2}}^{\frac{h}{2} - \frac{h_0}{2}} \rho_j^i (1, z, z^2, \Phi(z), \Phi^2(z), z \Phi(z)) dz + \int_{\frac{h}{2} - \frac{h_0}{2}}^{\frac{h}{2}} \rho_j^i (1, z, z^2, \Phi(z), \Phi^2(z), z \Phi(z)) dz \quad (26)$$

3.4 Work done by external works

In this study, it is assumed that the micro plates rested in an orthotropic elastic medium and initial stresses are applied in length direction of each micro plate. Thus, work done by external work described as the following form (Kultu and Omurtag 2012, Mohammadimehr *et al.* 201)

$$V = V_{foundation} + V_{prestresload} = \frac{1}{2} \int_A \left[F_i^{elastic} w_i - N_{0x} \left(\frac{\partial w}{\partial x} \right)^2 \right] dA \quad (27)$$

where $V_{foundation}$ and $V_{prestresload}$ are the work done by orthotropic elastic foundation and initial stresses, respectively. Moreover, the elastic medium forces are presented as follows (Kultu and Omurtag 2012)

$$\left\{ \begin{aligned} F_1^{elastic} &= K_w w^{(1)} - K_{G\zeta} (\cos^2 \theta \frac{\partial^2 w^{(1)}}{\partial x^2} + 2 \cos \theta \sin \theta \frac{\partial^2 w^{(1)}}{\partial x \partial y} + \sin^2 \theta \frac{\partial^2 w^{(1)}}{\partial y^2}) \\ & - K_{G\eta} (\sin^2 \theta \frac{\partial^2 w^{(1)}}{\partial x^2} - 2 \cos \theta \sin \theta \frac{\partial^2 w^{(1)}}{\partial x \partial y} + \cos^2 \theta \frac{\partial^2 w^{(1)}}{\partial y^2}) \\ F_2^{elastic} &= K_w w^{(2)} - K_{G\zeta} (\cos^2 \theta \frac{\partial^2 w^{(2)}}{\partial x^2} + 2 \cos \theta \sin \theta \frac{\partial^2 w^{(2)}}{\partial x \partial y} + \sin^2 \theta \frac{\partial^2 w^{(2)}}{\partial y^2}) \\ & - K_{G\eta} (\sin^2 \theta \frac{\partial^2 w^{(2)}}{\partial x^2} - 2 \cos \theta \sin \theta \frac{\partial^2 w^{(2)}}{\partial x \partial y} + \cos^2 \theta \frac{\partial^2 w^{(2)}}{\partial y^2}) \\ F_3^{elastic} &= K_w (w^{(1)} - w^{(2)}) - K_{G\zeta} \left(\cos^2 \theta \frac{\partial^2 w^{(1)}}{\partial x^2} - \frac{\partial^2 w^{(2)}}{\partial x^2} + 2 \cos \theta \sin \theta \left(\frac{\partial^2 w^{(1)}}{\partial x \partial y} - \frac{\partial^2 w^{(2)}}{\partial x \partial y} \right) \right. \\ & \left. + \sin^2 \theta \left(\frac{\partial^2 w^{(1)}}{\partial y^2} - \frac{\partial^2 w^{(2)}}{\partial y^2} \right) \right) \\ & - K_{G\eta} \left(\sin^2 \theta \left(\frac{\partial^2 w^{(1)}}{\partial x^2} - \frac{\partial^2 w^{(1)}}{\partial x^2} \right) - 2 \cos \theta \sin \theta \left(\frac{\partial^2 w^{(1)}}{\partial x \partial y} - \frac{\partial^2 w^{(1)}}{\partial x \partial y} \right) + \cos^2 \theta \left(\frac{\partial^2 w^{(1)}}{\partial y^2} - \frac{\partial^2 w^{(1)}}{\partial y^2} \right) \right) \end{aligned} \right\} \quad (28)$$

In the Eq. (28), $K_w, K_{G\zeta}, K_{G\eta}$ and θ are the Winkler spring constant, Pasternak shear modulus in the local directions and the angle of local direction, respectively. Also, (Mohammadimehr *et al.* 2017)

$$N_x^{prestresload} = \int_0^d N_{0x} w_{0,x} dx \quad ; \quad N_{0x} = \sigma_x A \quad (29)$$

where σ_x and A introduce the initial stresses and cross-section of surface plate, respectively.

Finally, by substituting Eqs. (28)-(29) into the Eq. (27) and applying the variation method, the first variation of work done by external works can be calculated as follows

$$\delta V = \int_A \left\{ \begin{aligned} & F_1^{elastic} \delta w_0^{(1)} + F_2^{elastic} (\delta w_0^{(1)} - \delta w_0^{(2)}) + F_3^{elastic} \delta w_0^{(2)} + N_x^{prestresload} \delta w_0^{(1)} + N_x^{prestresload} \delta w_0^{(2)} dA \\ & \left[K_w w^{(1)} + K_w (w_0^{(1)} - w_0^{(2)}) + (-K_{G\zeta} \cos^2 \theta - K_{G\eta} \sin^2 \theta) (\Delta w_{0,xx}^{(1)} - w_{0,xx}^{(2)}) \right. \\ & \left. + (-2K_{G\zeta} \cos \theta \sin \theta + 2K_{G\eta} \cos \theta \sin \theta) (\Delta w_{0,xy}^{(1)} - w_{0,xy}^{(2)}) \right] \delta w_0^{(1)} \\ & + \left[(-K_{G\zeta} \sin^2 \theta - K_{G\eta} \cos^2 \theta) (\Delta w_{0,yy}^{(1)} - w_{0,yy}^{(2)}) + N_x w_{0,xx}^{(1)} \right. \\ & \left. - K_w w^{(2)} + K_w (w_0^{(2)} - w_0^{(1)}) + (-K_{G\zeta} \cos^2 \theta - K_{G\eta} \sin^2 \theta) (\Delta w_{0,xx}^{(2)} - w_{0,xx}^{(1)}) \right] \delta w_0^{(2)} \\ & + \left[(-2K_{G\zeta} \cos \theta \sin \theta + 2K_{G\eta} \cos \theta \sin \theta) (\Delta w_{0,xy}^{(2)} - w_{0,xy}^{(1)}) \right. \\ & \left. + (-K_{G\zeta} \sin^2 \theta - K_{G\eta} \cos^2 \theta) (\Delta w_{0,yy}^{(2)} - w_{0,yy}^{(1)}) + N_x w_{0,xx}^{(2)} \right] \delta w_0^{(2)} \end{aligned} \right\} dA \quad (30)$$

3.5 2D axial buckling load

In this article, it is assumed that 2D axial buckling load are applied in the length and width directions of double-bonded micro composite sandwich SSDT plates reinforced by CNTs and BNNTs that they are showed with N_{x0} and N_{y0} in x and y -directions, respectively. In order to considering the effect of axial buckling load, Eq. (31) can be written as follows (Mantari and Monge 2016, Mosallaie Barzoki *et al.* 2012)

$$\begin{cases} W_{ext}^x = \frac{1}{2} \int_0^a N_{x0} \left(\frac{\partial W}{\partial x} \right)^2 dx \\ W_{ext}^y = \frac{1}{2} \int_0^b N_{y0} \left(\frac{\partial W}{\partial y} \right)^2 dy \end{cases} \Rightarrow \begin{cases} \delta W_{ext}^x = - \int_0^a N_{x0} \frac{\partial^2 W}{\partial x^2} \delta W dx \\ \delta W_{ext}^y = - \int_0^b N_{y0} \frac{\partial^2 W}{\partial y^2} \delta W dy \end{cases} \quad (31)$$

It is noted that the axial buckling load in y -direction are considered as a coefficient of axial buckling load in x -direction and defined as follows

$$\begin{aligned} & \left[[K] - N_{x0} [N] \right] = 0 \\ & \alpha_{buck} = \frac{N_{y0}}{N_{x0}} \end{aligned} \quad (32)$$

3.6 The governing equations of motions

After defining the equations of potential energy, kinetic energy and work done by orthotropic elastic medium and initial stresses, the governing equations of double-bonded micro composite sandwich SSDT plates reinforced by CNTs and BNNTs rested in an orthotropic foundation under initial stresses and electro-magneto-mechanical loadings are obtained Hamilton's principle (Mohammadimehr and Mehrabi 2017)

$$\delta \left(\int_0^t (\mathcal{T} - U - V) dt \right) = 0 \Rightarrow \delta U + \delta V - \delta T = 0 \quad (33)$$

Substituting Eqs. (19), (25) and (30) into the Eq. (33) lead to define the governing equations of motions that they are defined in Appendix A.

4. Semi-analytical solution method

In the present study, in order to solve the governing equations of motions of double-bonded micro composite SSDT sandwich plates reinforced by CNTs and BNNTs, the Navier's solution method is employed for simply supported boundary conditions and calculated the natural frequencies and critical buckling load of microplates using stiffness, buckling and mass matrices and solving the eigenvalue problem. Thus, based on the Naviers' type method the displacement, magnetic and electric field variables are considered as a function of Fourier expansion and described as the following form (Mohammadimehr *et al.* 2017, 2016d)

$$u_0(x, y, t) = \sum_{n=1}^{\infty} \sum_{m=1}^{\infty} U_{mn} \cos\left(\frac{m\pi}{a}x\right) \sin\left(\frac{n\pi}{b}y\right) e^{i\omega t} \quad (34a)$$

$$v_0(x, y, t) = \sum_{n=1}^{\infty} \sum_{m=1}^{\infty} V_{mn} \sin\left(\frac{m\pi}{a}x\right) \cos\left(\frac{n\pi}{b}y\right) e^{i\omega t} \quad (34b)$$

$$w_0(x, y, t) = \sum_{n=1}^{\infty} \sum_{m=1}^{\infty} W_{mn} \sin\left(\frac{m\pi}{a}x\right) \sin\left(\frac{n\pi}{b}y\right) e^{i\omega t} \quad (34c)$$

$$\theta_x(x, y, t) = \sum_{n=1}^{\infty} \sum_{m=1}^{\infty} \theta_{xmn} \cos\left(\frac{m\pi}{a}x\right) \sin\left(\frac{n\pi}{b}y\right) e^{i\omega t} \quad (34d)$$

$$\theta_y(x, y, t) = \sum_{n=1}^{\infty} \sum_{m=1}^{\infty} \theta_{ymn} \sin\left(\frac{m\pi}{a}x\right) \cos\left(\frac{n\pi}{b}y\right) e^{i\omega t} \quad (34e)$$

$$\phi_H(x, y, t) = \sum_{n=1}^{\infty} \sum_{m=1}^{\infty} \phi_{Hmn} \sin\left(\frac{m\pi}{a}x\right) \sin\left(\frac{n\pi}{b}y\right) e^{i\omega t} \quad (34f)$$

$$\phi_E(x, y, t) = \sum_{n=1}^{\infty} \sum_{m=1}^{\infty} \phi_{Emn} \sin\left(\frac{m\pi}{a}x\right) \sin\left(\frac{n\pi}{b}y\right) e^{i\omega t} \quad (34g)$$

where U_{mn} , V_{mn} , W_{mn} , θ_{xmn} , θ_{ymn} , ϕ_{Hmn} and ϕ_{Emn} are the undetermined Fourier coefficient, respectively. Also, m , n and ω refer to the transverse wave numbers in various directions and natural frequencies, respectively.

Moreover, the simply supported boundary condition in $x=0$, $x=a$, $y=0$ and $y=b$ can be given as follows

$$\begin{aligned} x=0 \rightarrow & \begin{cases} W=0 \\ M_y=0 \Rightarrow W_{,xx} + W_{,yy} = 0 \end{cases} ; & x=a \rightarrow & \begin{cases} W=0 \\ M_y=0 \Rightarrow W_{,xx} + W_{,yy} = 0 \end{cases} \\ y=0 \rightarrow & \begin{cases} W=0 \\ M_x=0 \Rightarrow W_{,xx} + W_{,yy} = 0 \end{cases} ; & y=b \rightarrow & \begin{cases} W=0 \\ M_x=0 \Rightarrow W_{,xx} + W_{,yy} = 0 \end{cases} \end{aligned} \quad (35)$$

5. Validation

In order to compare and validate the obtained results from sandwich formulation with the other previous researches, this section gives a comparison of the natural frequencies of a sandwich plate with aluminum face sheets and a soft orthotropic core.

Table 6 compares the numerical results between the present study and Larbi's *et al.* (2016), Ferreira's *et al.* (2013), Araújo's *et al.* (2010) and Rikard's *et al.* (1993) works. The data from this Table are obtained based on $E=70.23 \text{ Gpa}$, $\nu=0.3$ and $\rho=2820 \text{ Kg/m}^3$ for the aluminum face sheets and $E_1=E_2=137 \text{ Mpa}$, $G_{12}=45.7 \text{ Mpa}$, $G_{13}=137 \text{ Mpa}$, $G_{23}=52.7 \text{ Mpa}$, $\nu_{12}=0.5$ and $\rho=124.1 \text{ Kg/m}^3$ for the orthotropic soft core. It is illustrated that there is a good agreement between the obtained results for the first ten natural frequencies.

6. Results and discussion

In this section, the effects of various parameters such as material length scale parameter, length to width and thickness ratios, thickness of face sheets to core thickness ratio, nanotubes volume fraction, pre-stress load and orthotropic elastic medium are considered on the natural frequencies and critical buckling load of double-bonded micro composite

Table 6 comparison of obtained first ten natural frequencies of a sandwich plate from the present study with the previous researches

Mode number	Natural frequencies (HZ)					
	Experimental tests [62]	Larbi <i>et al.</i> [44]	Ferreira <i>et al.</i> [12]	Araújo <i>et al.</i> [45]	Rikards <i>et al.</i> [46]	Present work
1		23.25	23.26	23.50	23.40	23.27
2	45.0	44.52	44.60	44.80	45.40	44.65
3	69.0	71.43	70.27	71.70	72.20	71.06
4	78.0	80.02	79.90	79.50	81.60	80.10
5	92.0	91.32	91.08	92.50	95.90	92.19
6	129.0	126.02	125.51	126.50	133.70	127.20
7	133.0	129.80	128.85	126.80	134.20	129.30
8	152.0	151.79	145.16	150.70	152.20	149.10
9	169.0	170.73	165.16	170.70	156.80	169.80
10	177.0	174.17	173.29	173.00	190.90	175.90

sandwich SSDT plates reinforced by CNTs and BNNTs. The used constants and parameters are described as follows

$$\begin{aligned}
 h=2l & & a=10h & & b=a & & h_1 = \frac{h_c}{2} = \frac{h}{4} & & l_0=l_1=l_2=l & & l=17.6 \mu m \\
 k_w=10(GN/m^3) & & k_C=10(KN/m^3) & & C_s=0.4(mN.sec/m) & & T_0=300K & & \Delta T=20
 \end{aligned}$$

Moreover, dimensionless natural frequencies and critical buckling load can be defined as follows (Mantari and Monge 2016, Mohammadimehr *et al.* 2016d)

$$\tilde{\omega} = \omega \frac{a^2}{h} \sqrt{\frac{\rho_m}{E_m}} \quad ; \quad \tilde{N}_{cr} = N_{cr} \frac{a^2}{100h^3 E_m} \tag{36}$$

where

$$\rho_m = 1150(kg / m^3) \quad ; \quad E_m = 2.1(Gpa) \tag{37}$$

Fig. 2 depicts the effects of material length scale parameter on the dimensionless natural frequency and critical buckling load of double-bonded micro composite sandwich SSDT plates. In this figure, the CT, most general couple stress theory (MGCST) and MGSST are compared and showed that the dimensionless natural frequency and critical buckling load decrease when the thickness to material length scale parameter ratio increases. In fact, it can be said that when h/l increases the microstructure stiffness reduces, thus dimensionless natural frequency and critical buckling load decrease. Also, it is shown that the effect of MGSST is more than the other theories because of in the MGSST the stiffness matrix is larger than MGCST and CT, thus increasing the stiffness of microplates lead to increase the natural frequency and critical buckling load for MGSST, while material length scale parameter had no effect on the classic theory.

Fig. 3 shows the effect of axial buckling loads in x and y -directions on the critical buckling load of double-bonded micro composite SSDT plates reinforced by CNTs and BNNTs and it should be important in each direction. Thus, the axial loads in plate width is considered as a coefficient of axial load in length direction and introduce with α . Therefore, it is seen that critical buckling load decreases with increasing α coefficient. On the other hands, when α enhances, axial buckling load convergence to 1D loading and lead to decrease

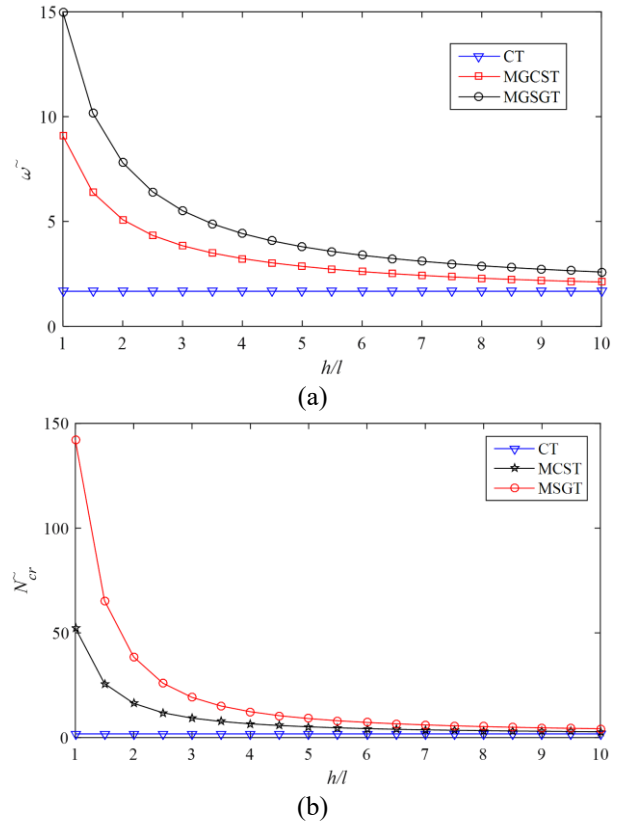


Fig. 2 Effects of material length scale parameter on the (a) dimensionless natural frequency (b) dimensionless critical buckling load of double-bonded micro composite SSDT plates versus thickness to material length scale ratio

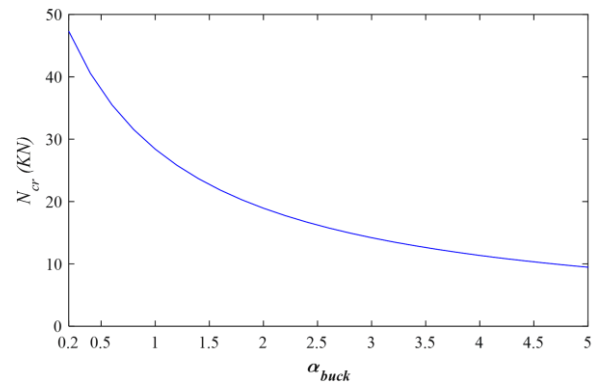


Fig. 3 Effects of axial loads ratio in x and y -directions on the critical buckling load of double-bonded micro composite SSDT plates reinforced by CNTs and BNNTs

stiffness of double-bonded plates and critical buckling load reduces by increasing the micro structure stiffness.

Fig. 4 illustrates role of reinforcement on the increasing stiffness of micro structures. As seen that the face sheets reinforced by CNTs and BNNTs have important effect on the vibration and buckling response of micro composite plates. In this figure, the cores of micro structure are considered as an orthotropic soft material and compared various value of volume fraction nanotube on the natural frequencies and critical buckling load of double-bonded micro sandwich SSDT plates. It is noted that in the present study, the upper

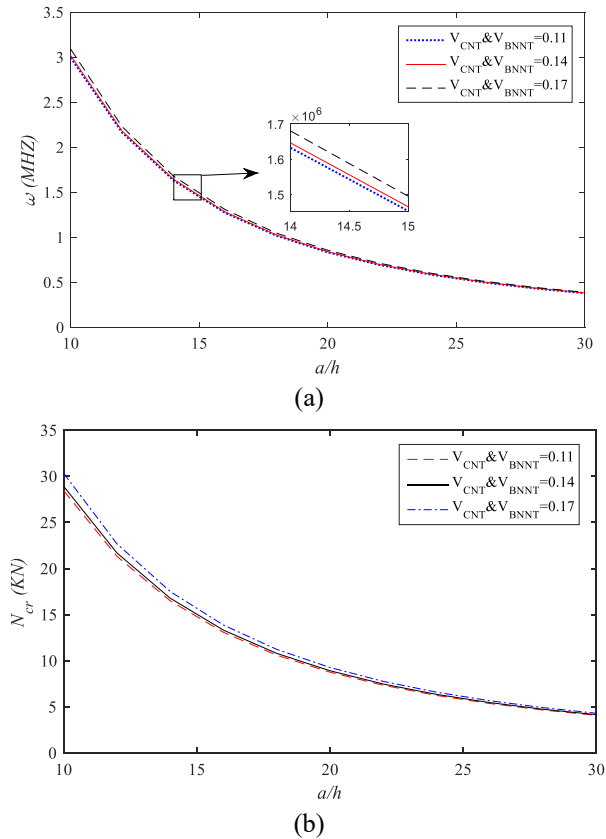


Fig. 4 Effects of CNTs and BNNTs volume fraction on the (a) natural frequency (b) critical buckling load of double-bonded micro composite SSDT plates based on orthotropic soft core

and lower micro composite plates reinforced by CNTs and BNNTs, respectively that the volume fraction of them are considered equal in each micro plate. Therefore, the natural frequencies and critical buckling load enhance when the volume fraction nanotubes lead to increase the micro structure stiffness. Also, it is showed that the natural frequencies and critical buckling load changes are not large because the orthotropic cores have large mechanical properties. But, when the isotropic foam core used in system, it observed that the natural frequency and critical buckling load is more change when the volume fraction nanotubes increases in Fig. 5. Moreover, it is showed that increasing length-to-thickness ratio lead to decrease the natural frequency and critical buckling load because micro structures stiffness reduces when enhance length of micro plate. So that these changes are important for the lower values of length-to-thickness ratios ($a/h < 25$).

Effects of aspect ratio and temperature changes on the natural frequencies and critical buckling load of double-bonded micro composite sandwich SSDT plates reinforced by CNTs and BNNTs are shown in Fig. 6. As seen that, the natural frequencies and critical buckling load of micro plates decrease with increasing of the aspect ratio because the micro structure stiffness reduces when the length-to-width ratio of micro plates enhances. In fact, when the aspect ratio increases, the micro structure becomes slender and these changes lead to

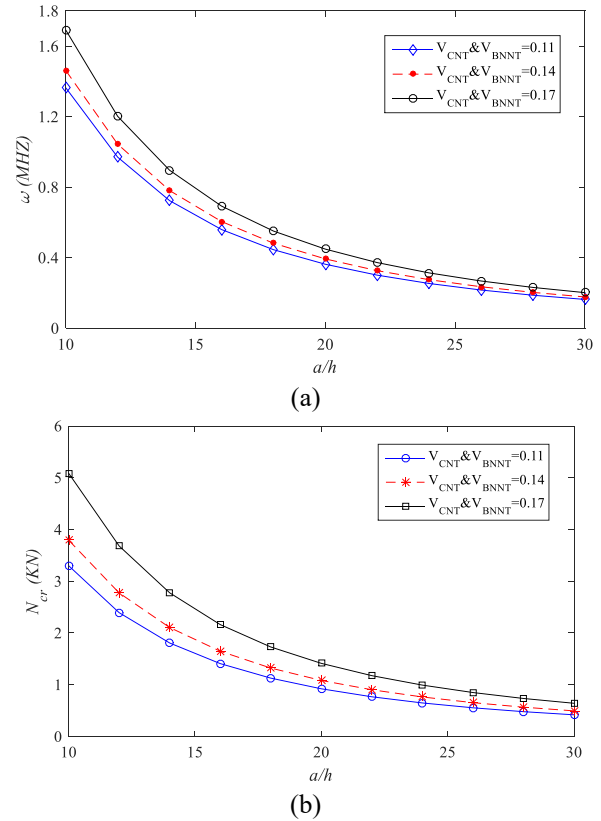


Fig. 5 Effects of CNTs and BNNTs volume fraction on the (a) natural frequency (b) critical buckling load of double-bonded micro composite SSDT plates based on isotropic foam core

decrease the micro plate stiffness. Moreover, it is observed that the temperature changes have a small effect on the buckling and vibration response of double-bonded micro composite sandwich plates with orthotropic cores. Since it is assumed that the cores are made of orthotropic materials with high stiffness, it can be expected that temperature changes are not very effective. But, influences of temperature changes were high when the isotropic foam core used as cores of microstructures (Fig. 7).

It is demonstrated that the effects of temperature changes are less for the cores with high stiffness, even though using the cores with large stiffness are not common in industries. Also, Fig. 7 illustrated the effects of thickness ratio (thickness of cores to face sheets stiffness) on the free vibration and buckling behaviors of double-bonded sandwich micro composite plates. In the sandwich structures because of low weight and high stiffness, usually, the face sheets are stiffer than cores. Thus, it is reasonable that buckling and resonance phenomenon delay when the stiffness is high by decreasing the thickness ratio. As seen that, the natural frequencies and critical buckling load of micro plates decrease with increasing the thickness ratio.

Table 7 compares the natural frequencies and critical buckling load of 1-layered double-bonded composite SSDT plates and 3-layered sandwich micro SSDT plates with orthotropic (large density and mechanical properties) and isotropic foam (low density and mechanical properties) cores. In this Table, all of the variables are same and changed the

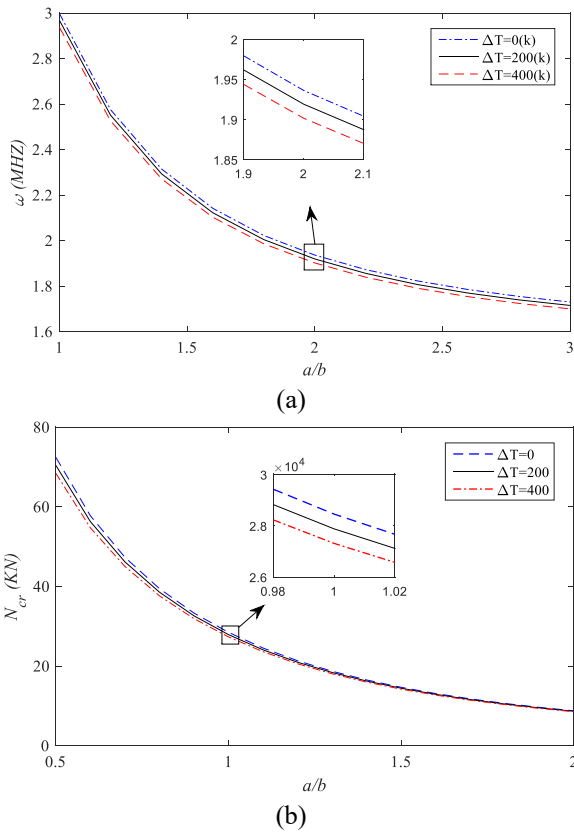


Fig. 6 Effects of aspect ratio and temperature changes on the (a) natural frequencies (b) critical buckling load of double-bonded micro composite SSDT plates based on orthotropic flexible cores

Table 7 comparison of natural frequencies and critical buckling load of double-bonded 1-layered, 3-layered with orthotropic and 3-layered with isotropic foam cores composite micro SSDT plates

	Slender Ratio (a/h)	1-layered composite micro structure	3-layered sandwich micro structure with orthotropic cores	3-layered sandwich micro structure with isotropic cores	$E_{Orto-Comp}$	$E_{Fom-Comp}$
Natural Frequency (HZ)	10	56771.900	138600.000	58912.200	1.440	0.037
	20	14445.400	34852.200	14772.100	1.410	0.022
	30	6570.940	15506.800	6569.020	1.350	0.00015
Critical Buckling Load (N)	10	812.719	1505.970	150.963	0.853	4.377
	20	210.372	380.644	37.932	0.814	4.526
	30	97.943	169.582	16.879	0.734	4.764

$$E_{Orto-Comp} = \frac{A_{Orto} - A_{Comp}}{A_{Comp}} \quad A : (\omega, N_{cr})$$

$$E_{Fom-Comp} = \frac{A_{Fom} - A_{Comp}}{A_{Comp}} \quad A : (\omega, N_{cr})$$

cores structures only with reinforced composite (1-layered), orthotropic and isotropic foam core. It is showed that in the double-bonded 3-layered sandwich micro plates with orthotropic cores the natural frequencies and critical buckling load are very large because these cores have high stiffness and mechanical properties.

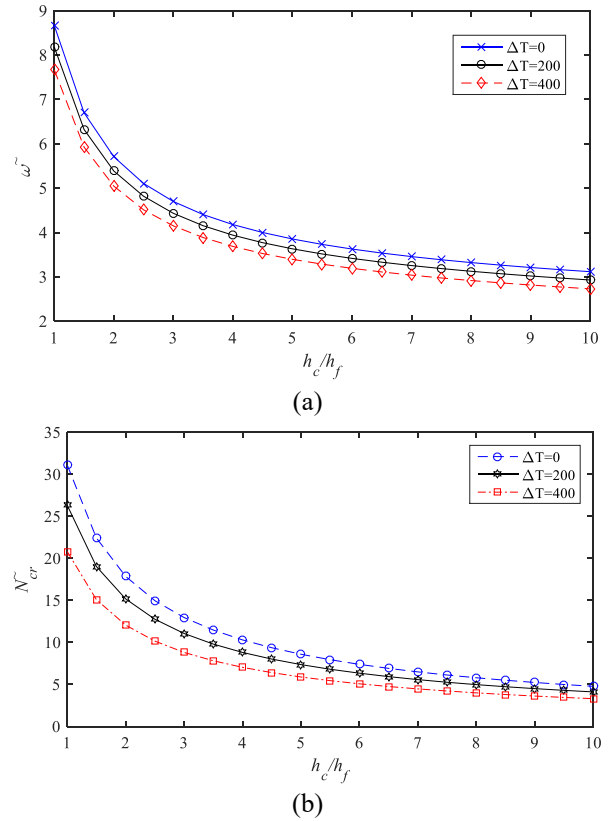


Fig. 7 Effects of temperature changes on the a) natural frequencies b) critical buckling load of double-bonded micro composite SSDT plates based on isotropic foam cores versus thickness ratio

Fig. 8 illustrated role of orthotropic elastic medium on the natural frequencies and critical buckling load of double-bonded micro composite sandwich SSDT plates with orthotropic core materials. It is observed that the micro structure stiffness increases with considering the elastic medium because the natural frequencies and critical buckling load of double-bonded micro sandwich plates enhances when the Winkler constant and Pasternak shear modulus increases. In fact, it can be said that the orthotropic foundation represents the environment elasticity around each micro sandwich plates and using this foundation lead to increase stability of micro system. Thus, the natural frequencies and critical buckling load increase with increasing the medium constants. Also, it is shown that the effect of Winkler spring constant is significant for $K_w \geq 10^{11} (N / m^3)$. In fact, in order to control the vibration and buckling response of double-bonded micro sandwich SSDT plates reinforced by CNTs and BNNTs the best domain will be $100 \leq K_w \leq 10000 (GN / m^3)$ because the most changes are occurred in this range. Moreover, the influences of Pasternak shear modulus are investigated in this figure, so that increasing the Pasternak shear modulus leads to enhance the natural frequencies and critical buckling load of sandwich micro SSDT plates. It is observed that the effect of this parameter is more than Winkler spring constant.

In this work, it is assumed that the tensile and compressive pre-stresses (positive and negative pre-stress load, respectively) are applied in x-direction of each micro

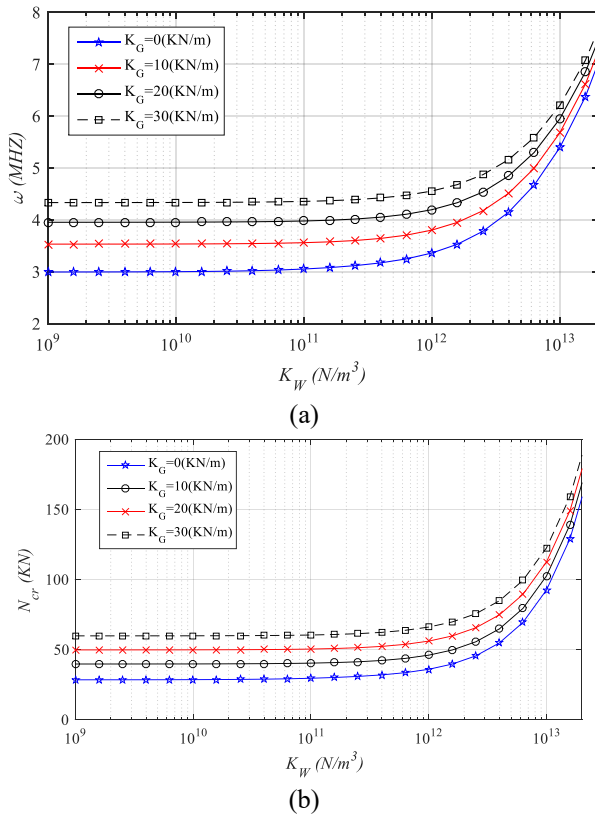


Fig. 8 Effects of orthotropic elastic medium constant on the (a) natural frequencies (b) critical buckling load of double-bonded micro composite sandwich SSDT plates with orthotropic cores

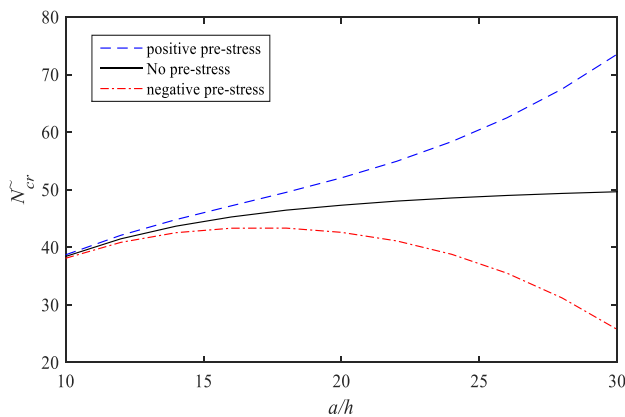


Fig. 9 Effects of pre-stress load in x -direction on the dimensionless critical buckling load of double-bonded micro composite sandwich SSDT plates ($\sigma_0 = 1e14(N/m^2) \rightarrow N_x = 11.5(KN)$)

sandwich SSDT plates reinforced by CNTs and BNNTs. Fig. 9. shows the effect of pre-stresses load on the dimensionless critical buckling load of present micro structure. It is concluded that the pre-stress load has an external factor on the buckling response of system and lead to increase the dimensionless critical buckling load, if this stress is applied tensile, while negative pre-stresses lead to decrease the critical buckling load. Thus, when the compressive pre-stresses load applied, the buckling phenomenon occurred earlier.

7. Conclusions

In this work, the buckling and free vibration analyses of double-bonded micro composite sandwich SSDT plates presented based on MSGT rested on an orthotropic medium under electro-magneto-thermo-mechanical and pre-stresses loadings. The sandwich micro plates considered with four composite face sheets and two flexible transversely orthotropic cores. Also, assumed that the face sheets material properties were temperature-dependent and they reinforced by CNTs and BNNTs. The governing equations of motions derived using Hamilton's principle and energy approach. Effects of various parameters such as material length scale parameter, length to width ratio, length-to-thickness ratio, and thickness of face sheets-to-core thickness ratio, nanotubes volume fraction, pre-stress load and orthotropic elastic medium on the natural frequencies and critical buckling load of double-bonded micro composite sandwich plates considered and the obtained results are stated as follows:

1) Influence of the Pasternak shear modulus is more than the Winkler spring constant on the critical buckling load and natural frequencies of double-bonded micro composite sandwich SSDT plates. So that, the critical buckling load and natural frequency of micro plates increase with increasing of both them.

2) CNTs and BNNTs volume fraction led to enhance the stiffness of micro composite sandwich plates and increases system stability.

3) Natural frequencies and critical buckling load of double-bonded micro composite sandwich SSDT plates decreases with increasing temperature changes. Moreover, temperature changes influence on the structural behaviors was less important compared to the other parameters.

4) Increasing length-to-thickness ratio of double-bonded micro SSDT plates led to decrease the natural frequencies and critical buckling load of system. Thus, it can be said that the buckling and resonance phenomenon occurs earlier when the micro plates are long.

5) Compressive pre-stresses due to help the axial buckling load causes that delay the buckling phenomenon.

6) Sandwich structures with orthotropic cores have high stiffness, but because they are not economical it is necessary the sandwich plates with foam core reinforce by CNTs and BNNTs because these nanotubes have important thermal and mechanical properties in comparison the other reinforcement.

Acknowledgments

The authors would like to thank the referees for their valuable comments. Also, they are thankful to the Iranian Nanotechnology Development Committee for their financial support and the University of Kashan for supporting this work by Grant No. 682561/2.

References

Akbari Alashti, R. and Khorsand, M. (2012), "Three-dimensional dynamo-thermo-elastic analysis of a functionally graded cylindrical shell with piezoelectric layers by DQ-FD coupled",

- J. Pre.Vessel. Pip.*, **96**, 49-67.
- Ansari, R., Faghhi Shojaei, M. and Rouhi, H. (2015), "Small-scale Timoshenko beam element", *Eur. J. Mech. A/Sol.*, **53**, 19-33.
- Ansari, R., Gholami, R., Faghhi Shojaei, M., Mohammadi, V. and Sahmani, S. (2013), "Size-dependent bending, buckling and free vibration of functionally graded Timoshenko micro beams based on the most general strain gradient theory", *Compos. Struct.*, **100**, 385-397.
- Araújo, A.L., MotaSoares, C.M. and MotaSoares, C.A. (2010), "Finite element model for hybrid active-passive damping analysis of anisotropic laminated sandwich structures", *J. Sandw. Struct. Mater.*, **12**, 397-419.
- Bahaadini, R., Hosseini, M. and Jamalpoor, A. (2017), "Nonlocal and surface effects on the flutter instability of cantilevered nanotubes conveying fluid subjected to follower forces", *Phys. B*, **509**, 55-61.
- Bahadori, R. and Najafzadeh, M.M. (2015), "Free vibration analysis of two-dimensional functionally graded axisymmetric cylindrical shell on Winkler-Pasternak elastic foundation by first-order shear deformation theory and using navier-differential quadrature solution methods", *Appl. Math. Model.*, **139**, 4877-4894.
- Batra, R.C., Porfiri, M. and Spinell, D. (2008a), "Vibrations of narrow micro beams predeformed by an electric field", *J. Sound Vibr.*, **309**, 600-612.
- Batra, R.C., Porfiri, M. and Spinell, D. (2008b), "Vibrations and pull-in instabilities of micro electro mechanical Von Karman elliptic incorporating the casimir force", *J. Sound Vibr.*, **315**, 939-960.
- Botshekanan Dehkordi, M., Cinefra, M., Khalili, S.M.R. and Carrera, E. (2013), "Mixed LW/WSL models for the analysis of sandwich plates with composite faces", *Compos. Struct.*, **98**, 330-339.
- Chakrabarti, A., Mukhopadhyay, B. and Bera, R.K. (2007), "Nonlinear stability of a shallow unsymmetrical heated orthotropic sandwich shell of double curvature with orthotropic core", *J. Sol. Struct.*, **44**, 5412-5424.
- Chen, X. and Feng, Z. (2017), "Dynamic behavior of a thin laminated plate embedded with auxetic layers subject to in-plane excitation", *Mech. Res. Comm.*, **85**, 45-52.
- Civalek, Ö., Demir, C. and Akgöz, B. (2009), "Static analysis of single walled carbon nanotubes (SWCNT) based on Eringen's nonlocal elasticity theory", *J. Engin. Appl. Sci.*, **2**, 47-56.
- Dai, H.L., Zhao, D.M., Zou, J.J. and Wang, L. (2016), "Surface effect on the nonlinear forced vibration of cantilevered nanobeams", *Phys. E*, **80**, 25-30.
- Ergun, E., Yilmaz, Y. and allioglu, H. (2016), "Free vibration and buckling analysis of the impacted hybrid composite beams", *Struct. Eng. Mech.*, **59**, 1055-1070
- Farajpour, A., Rastgoo, A. and Mohammadi, M. (2017), "Vibration, buckling and smart control of microtubules using piezoelectric nanoshells under electric voltage in thermal environment", *Phys. B*, **509**, 100-114.
- Ferreira, A.J.M., Araújo, A.L., Neves, A.M.A., Rodrigues, J.D., Carrera, E., Cinefra, M. and Soares, C.M. (2013), "A finite element model using a unified formulation for the analysis of viscoelastic sandwich laminates", *Compos. B*, **45**, 1258-1264.
- Ghorbanpour Arani, A. and Zamani, M.H. (2017), "Investigation of electric field effect on size-dependent bending analysis of functionally graded porous shear and normal deformable sandwich nanoplate on silica aerogel foundation", *J. Sandw. Struct. Mater.*
- Ghorbanpour Arani, A., Khani Arani, H and Khoddami Maraghi, Z. (2016), "Vibration analysis of sandwich composite micro plate under electro-magneto-mechanical loadings", *Appl. Math. Model.*, **40**, 10596-10615.
- Ghorbanpour Arani, A., Shajari, A.R., Amir, S. and Loghman, A. (2012), "Electro-thermo-mechanical nonlinear nonlocal vibration and instability of embedded micro-tube reinforced by BNNT, conveying fluid", *Phys. E*, **45**, 109-121.
- Kaghazian, A., Hajnayeb, A. and Foruzande, H. (2017), "Free vibration analysis of a piezoelectric nanobeam using nonlocal elasticity theory", *Struct. Eng. Mech.*, **6**, 617-624.
- Ke, L.L., Wang, Y.Sh. Yang, J. and Kitipornchai, S. (2012), "Free vibration of size-dependent Mindlin micro plates based on modified couple stress theory", *J. Sound Vibr.*, **331**, 94-106.
- Kolahchi, R., Zarei, M.S., Hajmohammad, M.H. and Oskouei, A.N. (2017), "Visco-nonlocal-refined Zigzag theories for dynamic buckling of laminated nanoplates using differential cubature-Bolotin methods", *Thin Wall. Struct.*, **113**, 162-169.
- Kutlu, A. and Omurtag, M.H. (2012), "Large deflection bending analysis of elliptic plates on orthotropic elastic foundation with mixed finite element method", *J. Mech. Sci.*, **65**, 64-74.
- Larbi, W., Deü, J.F. and Ohayon, R. (2016), "Vibroacoustic analysis of double-wall sandwich panels with viscoelastic core", *Comput. Struct.*, **174**, 92-103.
- Lau, A.K.T. and Hui, D. (2002), "The revolutionary creation of new advanced materials- carbon nanotube composites", *Compos. B*, **33**, 263-277.
- Lei, Z.X., Liew, K.M. and Yu, J.L. (2013), "Buckling analysis of functionally graded carbon nanotube-reinforced composite plates using the element-free kp-ritz method", *Compos. Struct.*, **98**, 160-168.
- Li, D.H., Wang, R.P., Qian, R.L., Liu, Y. and Qing, G.H. (2016), "Static response and free vibration analysis of the composite sandwich structures with multi-layer cores", *J. Mech. Sci.*, **111-112**, 101-115.
- Mantari, J.L. and Monge, J.C. (2016), "Buckling, free vibration and bending analysis of functionally graded sandwich plates based on an optimized hyperbolic unified formulation", *J. Mech. Sci.*, **119**, 170-186.
- Mirjavadi, S.S., Rabby, S., Shafiei, N., MohaselAfshar, B. and Kazemi, M. (2017), "on size-dependent free vibration and thermal buckling of axially functionally graded nanobeams in thermal environment", *Appl. Phys. A*, **123**, 315-325.
- Mirsalehi, M., Azhari, M. and Amoushahi, H. (2017), "Buckling and free vibration of the FGM thin micro-plate based on the modified strain gradient theory and the spline finite strip method", *Eur. J. Mech. A/Sol.*, **61**, 1-13.
- Mohammadimehr, M. and Alimirzaei, S. (2016a), "Nonlinear static and vibration analysis of Euler-Bernoulli composite beam model reinforced by FG-SWCNT with initial geometrical imperfection using FEM", *Struct. Eng. Mech.*, **59**(3), 431-454.
- Mohammadimehr, M. and Mehrabi, M. (2017), "Stability and vibration analysis of double-bonded micro composite sandwich cylindrical shells conveying fluid flow", *Appl. Math. Model.*, **47**, 685-709.
- Mohammadimehr, M., Mohammadi Hooyeh, H., Afshari, H. and Salarkia, M.R. (2017), "Free vibration analysis of double-bonded isotropic piezoelectric Timoshenko microbeam based on strain gradient and surface stress elasticity theories under initial stress using differential quadrature method", *Mech. Adv. Mater. Struct.*, **24**(4), 287-303.
- Mohammadimehr, M., Mohandes, M. and Moradi, M. (2016b), "Size dependent effect on the buckling and vibration analysis of double-bonded nanocomposite piezoelectric plate reinforced by boron nitride nanotube based on modified couple stress theory", *J. Vib. Contr.*, **22**, 1790-1807.
- Mohammadimehr, M., Okhravi, S.V. and Akhavan Alavi, S.M. (2016c), "Free vibration analysis of magneto-electro-elastic cylindrical composite panel reinforced by various distributions of CNTs with considering open and closed circuits boundary conditions based on FSDT", *J. Vib. Contr.*, 1-9.
- Mohammadimehr, M., Salemi, M. and Roustavi Navi, B. (2016d),

“Bending, buckling and free vibration analysis of MSGT micro composite reddy plate reinforced by FG-SWCNTs with temperature-dependent material properties under hydro-thermo-mechanical loadings using DQM”, *Compos. Struct.*, **138**, 361-380.

MosallaieBarzoki, A., GhorbanpourArani, A., Kolahchi, R. and Mozdianfard, M.R. (2012), “Electro-thermo-mechanical torsional buckling of a piezoelectric polymeric cylindrical shell reinforced by DWBNTs with an elastic core”, *Appl. Math. Model*, **36**, 2983-2995.

Nasihatgozar, M., Daghigh, V., Eskandari, M., Nikbin, K. and Simoneau, A. (2016), “Buckling analysis of piezoelectric cylindrical composite panels reinforced with carbon nanotubes”, *J. Mech. Sci.*, **107**, 69-79.

Reissner, E. (1948), “Finite deflections of sandwich plates”, *J. Aero. Sci.*, **15**, 435-440.

Rikards, R., Chate, A. and Barkanov, E. (1993), “Finite element analysis of damping the vibrations of laminated composites”, *Comput. Struct.*, **47**, 1005-1015.

Robin, G., Mathieu, N., Jrad, M., Daya, E.M. and Choquart, F. (2017), “The effect of the geometric parameters of the corrugation shape on the vibration analysis of 3D structured beams”, *Mech. Res. Comm*, **84**, 65-71.

Rouhi, H., Ansari, R. and Darvizeh, M. (2016), “Size-dependent free vibration analysis of nano shells based on the surface stress elasticity”, *Appl. Math. Model*, **40**, 3128-3140.

Shen, H., Wang, H. and Yang, D. (2017), “Vibration of thermally post-buckled sandwich plates with nanotube-reinforced composite face sheets resting on elastic foundation”, *J. Mech. Sci.*, **124-125**, 253-262.

Shooshtari, A. and Razavi, S. (2015), “Nonlinear vibration analysis of rectangular magneto-electro-elastic thin plates”, *J. Eng.*, **28**, 139-147.

Swaminathan, K. and Sangeetha, D.M. (2017), “Thermal analysis of FGM plates-a critical review of various modelling techniques and solution methods”, *Compos. Struct.*, **160**, 43-60.

Thostenson, E.T., Ren, Z. and Chou, T.W. (2001), “Advances in the science and technology of carbon nanotubes and their composites: a review”, *Compos. Sci. Technol.*, **61**, 1899-1912.

Wang, W.L. and Hu, S.J. (2005), “Modal response and frequency shift of the cantilever in a noncontact atomic force microscope”, *Appl. Phys. Lett.*, **87**, 183-506.

Wang, Y.G., Song, H.F., Lin, W.H. and Xu, L. (2017), “Large deflection analysis of functionally graded circular microplates with modified couple stress effect”, *J. Braz. Soc. Mech. Sci. Eng.*, **39**, 981-991.

Xu, X., Rong, D., Lim, C.W., Yang, C. and Zhou, Z. (2017), “An analytical symplectic approach to the vibration analysis of orthotropic graphene sheets”, *Acta. Sinica*, 1-14.

Yan, J.B. and Richard Liew, J.Y. (2016), “Design and behavior of steel-concrete-steel sandwich plates subject to concentrated loads”, *Compos. Struct.*, **150**, 139-152.

Zhao, R., Yu, K., Hulbert, G.M., Wu, Y. and Li, X. (2017), “Piecewise shear deformation theory and finite element formulation for vibration analysis of laminated composite and sandwich plates in thermal environments”, *Compos. Struct.*, **160**, 1060-1083.

Zhu, P., Lei, Z.X. and Liew, K.M. (2012), “Static and free vibration analyses of carbon nano tube-reinforced composite plates using finite element method with first order shear deformation theory”, *Compos. Struct.*, **94**, 1450-1460.

Appendix A

The governing equations of motions can be defined by Substituting Eq. (19), (25) and (30) into Eq. (33). These equations are written as follows:

- The governing equations of motions of upper micro plate

$$\begin{aligned} \delta u_0^{(1)}: & -A_1^4 u_{0,xx}^{(1)} - A_1^4 u_{0,yy}^{(1)} + \alpha_1 s^{(0)} u_0^{(1)} + (2\alpha_5 + 2\alpha_4 + \alpha_3 + \alpha_7 + \alpha_9) s^{(0)} u_0^{(1)} + (\alpha_6 + \alpha_{12}) s^{(0)} u_{0,xy}^{(1)} \\ & + I_0^4 u_{0,xx}^{(1)} - (A_{12}^4 + A_{66}^4) v_{0,xy}^{(1)} + (\alpha_2 + \alpha_3 + \alpha_4 + \alpha_5) s^{(0)} v_{0,xy}^{(1)} + (\alpha_3 + \alpha_2 + \alpha_4 + \alpha_6 + \alpha_{12}) s^{(0)} v_{0,xy}^{(1)} \\ & - B_{12}^4 v_{0,xy}^{(1)} + (B_{12}^4 + 2B_{66}^4) w_{0,xy}^{(1)} - \alpha_1 s^{(1)} w_{0,xy}^{(1)} - (\alpha_2 + 3\alpha_3 + 3\alpha_4 + 2\alpha_5 + 2\alpha_7 + \alpha_9) s^{(1)} w_{0,xy}^{(1)} \\ & - (\alpha_4 + \alpha_2 + \alpha_6 + 2\alpha_7 + 2\alpha_{12}) s^{(1)} w_{0,xy}^{(1)} - I_1^4 w_{0,xy}^{(1)} + (-a_{11}^4 + \alpha_5 s^{(0)} s^{(1)}) \theta_{0,xx}^{(1)} + (-a_{66}^4 + \alpha_6 s^{(0)} s^{(1)}) \theta_{0,yy}^{(1)} \\ & + \alpha_5 s^{(R)} \theta_{0,xx}^{(1)} + (2\alpha_5 + 2\alpha_4 + \alpha_3 + \alpha_7 + \alpha_9) s^{(R)} \theta_{0,xx}^{(1)} + (\alpha_6 + \alpha_{12}) s^{(R)} \theta_{0,yy}^{(1)} + \alpha_6 s^{(R)} \theta_{0,yy}^{(1)} \\ & + R_1^4 \theta_{0,xx}^{(1)} + (-a_{11}^4 - a_{66}^4 + \alpha_6 s^{(R)} s^{(1)} + \alpha_5 s^{(R)} s^{(1)}) \theta_{0,xy}^{(1)} + (\alpha_2 + \alpha_3 + \alpha_4 + \alpha_5 + \alpha_7 + \alpha_9) s^{(R)} \theta_{0,xy}^{(1)} \\ & + (\alpha_3 + \alpha_2 + \alpha_4 + \alpha_6 + \alpha_{12}) s^{(R)} \theta_{0,xy}^{(1)} + N_{11}^4 + N_{12}^4 = 0 \end{aligned} \tag{A1}$$

$$\begin{aligned} \delta v_0^{(1)}: & (\alpha_4 + \alpha_3 + \alpha_2 + \alpha_6 + \alpha_9) s^{(0)} u_0^{(1)} + (\alpha_4 + \alpha_3 + \alpha_2 + \alpha_6 + \alpha_9) s^{(0)} u_0^{(1)} - (A_{66}^4 + A_{12}^4) w_{0,xy}^{(1)} - A_{12}^4 v_{0,xy}^{(1)} - A_{12}^4 v_{0,xy}^{(1)} \\ & + (2\alpha_5 + 2\alpha_4 + \alpha_3 + \alpha_7 + \alpha_9) s^{(0)} v_{0,xy}^{(1)} + (\alpha_5 + \alpha_7) s^{(0)} v_{0,xy}^{(1)} + \alpha_1 s^{(0)} v_{0,xy}^{(1)} + I_1^4 v_{0,xy}^{(1)} + (2B_{66}^4 + B_{12}^4) w_{0,xy}^{(1)} \\ & + B_{26}^4 w_{0,xy}^{(1)} - (A_{12}^4 + 2A_{66}^4) v_{0,xy}^{(1)} + \alpha_1 s^{(1)} v_{0,xy}^{(1)} + I_1^4 v_{0,xy}^{(1)} + D_{11}^4 v_{0,xy}^{(1)} + (D_{11}^4 + \alpha_5 s^{(0)} s^{(1)}) w_{0,xy}^{(1)} + (D_{12}^4 + 4D_{66}^4) \\ & + D_{21}^4 + 2\alpha_{66}^{(0)} + 4\alpha_{12}^{(0)} w_{0,xy}^{(1)} - (\alpha_2 + 3\alpha_3 + 3\alpha_4 + 2\alpha_5 + 2\alpha_7 + \alpha_9) s^{(2)} w_{0,xy}^{(1)} - (2\alpha_2 + 4\alpha_3 + 4\alpha_4 + 4\alpha_5 + 4\alpha_7 \\ & + \alpha_9) s^{(2)} w_{0,xy}^{(1)} - (4\alpha_3 + 4\alpha_4 + \alpha_5 + 2\alpha_7 + 4\alpha_9 + 4\alpha_{12}) s^{(2)} w_{0,xy}^{(1)} - I_1^4 w_{0,xy}^{(1)} - I_1^4 w_{0,xy}^{(1)} - I_1^4 w_{0,xy}^{(1)} + (K_{x1} \\ & + K_{x2}) w_{0,xy}^{(1)} - 2(K_{x2} \cos^2 \theta + K_{x1} \sin^2 \theta) w_{0,xy}^{(1)} - 4(K_{x2} \cos \theta \sin \theta) w_{0,xy}^{(1)} - 2(K_{x2} \sin^2 \theta + K_{x1} \cos^2 \theta) w_{0,xy}^{(1)} \\ & - N_{11}^{(1)} w_{0,xy}^{(1)} - (b_{11}^4 + \alpha_3 s^{(2R)} s^{(1)} - \alpha_5 s^{(2R)} s^{(1)} - \alpha_6 s^{(2R)} s^{(1)}) \theta_{0,xx}^{(1)} - (2b_{11}^4 + b_{21}^4 + \alpha_5 s^{(2R)} s^{(1)} + \alpha_6 s^{(2R)} s^{(1)} + 2\alpha_{12} s^{(2R)} s^{(1)} \\ & - \alpha_5 s^{(2R)} s^{(1)} - 2\alpha_6 s^{(2R)} s^{(1)}) \theta_{0,yy}^{(1)} + \alpha_1 s^{(2R)} \theta_{0,xx}^{(1)} + (\alpha_4 + 2\alpha_5 + 2\alpha_4 + \alpha_3 + \alpha_7 + \alpha_9) s^{(2R)} \theta_{0,xx}^{(1)} + (3\alpha_3 + 3\alpha_4 + 2\alpha_5 \\ & + 2\alpha_7 + \alpha_9 + \alpha_3) s^{(2R)} \theta_{0,yy}^{(1)} + IR_1^4 \theta_{0,xx}^{(1)} - (b_{12}^4 + 2b_{11}^4 - 2\alpha_{66}^{(2)} - \alpha_5 s^{(2R)} s^{(1)} + \alpha_6 s^{(2R)} s^{(1)} - \alpha_6 s^{(2R)} s^{(1)} \\ & + 2\alpha_{12} s^{(2R)} s^{(1)}) \theta_{0,xy}^{(1)} - (b_{12}^4 - \alpha_5 s^{(2R)} s^{(1)} + \alpha_6 s^{(2R)} s^{(1)}) \theta_{0,xy}^{(1)} + (\alpha_2 + \alpha_3 + 2\alpha_4 + 2\alpha_5 + 2\alpha_7 + \alpha_9) s^{(2R)} \theta_{0,xy}^{(1)} \\ & + (3\alpha_3 + 3\alpha_4 + \alpha_5 + 2\alpha_7 + 4\alpha_9 + 4\alpha_{12}) s^{(2R)} \theta_{0,xy}^{(1)} + \alpha_1 s^{(2R)} \theta_{0,xy}^{(1)} + M_{11}^4 + M_{12}^4 + M_{21}^4 + M_{22}^4 + IR_1^4 \theta_{0,xx}^{(1)} \\ & + K_{x1} w_{0,xy}^{(1)} + (K_{x2} \cos^2 \theta + K_{x1} \sin^2 \theta) w_{0,xy}^{(1)} + 2(K_{x2} \cos \theta \sin \theta) w_{0,xy}^{(1)} + (K_{x2} \sin^2 \theta + K_{x1} \cos^2 \theta) w_{0,xy}^{(1)} = 0 \end{aligned} \tag{A2}$$

$$\begin{aligned} \delta w_0^{(1)}: & -B_{12}^4 u_{0,xy}^{(1)} - (2B_{12}^4 - B_{21}^4) v_{0,xy}^{(1)} + \alpha_1 s^{(1)} u_0^{(1)} + (3\alpha_3 + 3\alpha_4 + 2\alpha_5 + 2\alpha_7 + \alpha_9) s^{(1)} u_0^{(1)} + (\alpha_4 + 2\alpha_5 + 2\alpha_4 \\ & + \alpha_2 + \alpha_3) s^{(1)} u_0^{(1)} + I_1^4 u_{0,xy}^{(1)} - (B_{12}^4 + 2B_{66}^4) v_{0,xy}^{(1)} + (\alpha_2 + \alpha_3 + \alpha_4 + \alpha_5 + \alpha_7 + \alpha_9) s^{(1)} v_{0,xy}^{(1)} + (3\alpha_3 + 3\alpha_4 + \alpha_5 + \alpha_7 + \alpha_9 \\ & + 2\alpha_5 + 2\alpha_4) s^{(1)} v_{0,xy}^{(1)} - B_{12}^4 v_{0,xy}^{(1)} + \alpha_1 s^{(1)} v_{0,xy}^{(1)} + I_1^4 v_{0,xy}^{(1)} + D_{11}^4 v_{0,xy}^{(1)} + (D_{11}^4 + \alpha_5 s^{(0)} s^{(1)}) w_{0,xy}^{(1)} + (D_{12}^4 + 4D_{66}^4) \\ & + D_{21}^4 + 2\alpha_{66}^{(0)} + 4\alpha_{12}^{(0)} w_{0,xy}^{(1)} - (\alpha_2 + 3\alpha_3 + 3\alpha_4 + 2\alpha_5 + 2\alpha_7 + \alpha_9) s^{(2)} w_{0,xy}^{(1)} - (2\alpha_2 + 4\alpha_3 + 4\alpha_4 + 4\alpha_5 + 4\alpha_7 \\ & + \alpha_9) s^{(2)} w_{0,xy}^{(1)} - (4\alpha_3 + 4\alpha_4 + \alpha_5 + 2\alpha_7 + 4\alpha_9 + 4\alpha_{12}) s^{(2)} w_{0,xy}^{(1)} - I_1^4 w_{0,xy}^{(1)} - I_1^4 w_{0,xy}^{(1)} - I_1^4 w_{0,xy}^{(1)} + (K_{x1} \\ & + K_{x2}) w_{0,xy}^{(1)} - 2(K_{x2} \cos^2 \theta + K_{x1} \sin^2 \theta) w_{0,xy}^{(1)} - 4(K_{x2} \cos \theta \sin \theta) w_{0,xy}^{(1)} - 2(K_{x2} \sin^2 \theta + K_{x1} \cos^2 \theta) w_{0,xy}^{(1)} \\ & - N_{11}^{(1)} w_{0,xy}^{(1)} - (b_{11}^4 + \alpha_3 s^{(2R)} s^{(1)} - \alpha_5 s^{(2R)} s^{(1)} - \alpha_6 s^{(2R)} s^{(1)}) \theta_{0,xx}^{(1)} - (2b_{11}^4 + b_{21}^4 + \alpha_5 s^{(2R)} s^{(1)} + \alpha_6 s^{(2R)} s^{(1)} + 2\alpha_{12} s^{(2R)} s^{(1)} \\ & - \alpha_5 s^{(2R)} s^{(1)} - 2\alpha_6 s^{(2R)} s^{(1)}) \theta_{0,yy}^{(1)} + \alpha_1 s^{(2R)} \theta_{0,xx}^{(1)} + (\alpha_4 + 2\alpha_5 + 2\alpha_4 + \alpha_3 + \alpha_7 + \alpha_9) s^{(2R)} \theta_{0,xx}^{(1)} + (3\alpha_3 + 3\alpha_4 + 2\alpha_5 \\ & + 2\alpha_7 + \alpha_9 + \alpha_3) s^{(2R)} \theta_{0,yy}^{(1)} + IR_1^4 \theta_{0,xx}^{(1)} - (b_{12}^4 + 2b_{11}^4 - 2\alpha_{66}^{(2)} - \alpha_5 s^{(2R)} s^{(1)} + \alpha_6 s^{(2R)} s^{(1)} - \alpha_6 s^{(2R)} s^{(1)} \\ & + 2\alpha_{12} s^{(2R)} s^{(1)}) \theta_{0,xy}^{(1)} - (b_{12}^4 - \alpha_5 s^{(2R)} s^{(1)} + \alpha_6 s^{(2R)} s^{(1)}) \theta_{0,xy}^{(1)} + (\alpha_2 + \alpha_3 + 2\alpha_4 + 2\alpha_5 + 2\alpha_7 + \alpha_9) s^{(2R)} \theta_{0,xy}^{(1)} \\ & + (3\alpha_3 + 3\alpha_4 + \alpha_5 + 2\alpha_7 + 4\alpha_9 + 4\alpha_{12}) s^{(2R)} \theta_{0,xy}^{(1)} + \alpha_1 s^{(2R)} \theta_{0,xy}^{(1)} + M_{11}^4 + M_{12}^4 + M_{21}^4 + M_{22}^4 + IR_1^4 \theta_{0,xx}^{(1)} \\ & + K_{x1} w_{0,xy}^{(1)} + (K_{x2} \cos^2 \theta + K_{x1} \sin^2 \theta) w_{0,xy}^{(1)} + 2(K_{x2} \cos \theta \sin \theta) w_{0,xy}^{(1)} + (K_{x2} \sin^2 \theta + K_{x1} \cos^2 \theta) w_{0,xy}^{(1)} = 0 \end{aligned} \tag{A3}$$

$$\begin{aligned} \delta \theta_0^{(1)}: & + (\alpha_5 + \alpha_3) s^{(0)} u_{0,xx}^{(1)} + (2\alpha_5 + 2\alpha_4 + \alpha_3 + \alpha_7 + \alpha_9) s^{(0)} u_{0,xx}^{(1)} + (\alpha_6 + \alpha_{12}) s^{(0)} u_{0,xx}^{(1)} + (-a_{11}^4 + \alpha_5 s^{(0)} s^{(1)}) \theta_{0,xx}^{(1)} \\ & + (\alpha_6 s^{(0)} s^{(1)} - a_{66}^4) \theta_{0,yy}^{(1)} + R_1^4 \theta_{0,xx}^{(1)} + (\alpha_5 s^{(R)} s^{(1)} + \alpha_6 s^{(R)} s^{(1)} - a_{11}^4) \theta_{0,xx}^{(1)} + (\alpha_5 + \alpha_7 + \alpha_9 + \alpha_3) s^{(R)} \theta_{0,xx}^{(1)} \\ & + (\alpha_3 + \alpha_2 + \alpha_4 + \alpha_6 + \alpha_{12}) s^{(R)} \theta_{0,yy}^{(1)} + (b_{11}^4 + \alpha_3 s^{(2R)} s^{(1)} + \alpha_5 s^{(2R)} s^{(1)} - \alpha_6 s^{(2R)} s^{(1)}) \theta_{0,xx}^{(1)} - \alpha_1 s^{(2R)} \theta_{0,xx}^{(1)} \\ & + (\alpha_5 s^{(R)} s^{(1)} + 2\alpha_6 s^{(R)} s^{(1)} + \alpha_6 s^{(R)} s^{(1)} + 2\alpha_{12} s^{(R)} s^{(1)} - \alpha_5 s^{(R)} s^{(1)} - 2\alpha_6 s^{(R)} s^{(1)} + b_{11}^4 + 2b_{12}^4) \theta_{0,xy}^{(1)} - (2\alpha_5 s^{(R)} s^{(1)} - d_{12}^4) \theta_{0,xy}^{(1)} \\ & + 2\alpha_4 + 2\alpha_5 + \alpha_3) s^{(R)} \theta_{0,xy}^{(1)} - (\alpha_3 + \alpha_2 + \alpha_4 + 2\alpha_5 + 2\alpha_7 + \alpha_9) s^{(R)} \theta_{0,xy}^{(1)} + (2\alpha_5 s^{(R)} s^{(1)} - \alpha_6 s^{(R)} s^{(1)} - d_{12}^4) \theta_{0,xy}^{(1)} \\ & - 2\alpha_5 s^{(R)} s^{(1)} - \alpha_6 s^{(R)} s^{(1)} - \alpha_6 s^{(R)} s^{(1)} - \alpha_6 s^{(R)} s^{(1)} - \alpha_6 s^{(R)} s^{(1)} - d_{11}^4) \theta_{0,xy}^{(1)} + (2\alpha_5 s^{(R)} s^{(1)} - 2\alpha_6 s^{(R)} s^{(1)} - 2\alpha_6 s^{(R)} s^{(1)} - d_{12}^4) \theta_{0,xy}^{(1)} \\ & + (2\alpha_4 + 2\alpha_5 + \alpha_3 + \alpha_7 + \alpha_9) s^{(R)} \theta_{0,xy}^{(1)} + (\alpha_3 + \alpha_2) s^{(R)} \theta_{0,xy}^{(1)} + \alpha_1 s^{(R)} \theta_{0,xy}^{(1)} + (\alpha_5 s^{(R)} s^{(1)} + \alpha_6 s^{(R)} s^{(1)} \\ & + \frac{1}{2} s^{(R)} s^{(1)}) \theta_{0,xx}^{(1)} + R_1^4 \theta_{0,xx}^{(1)} + (-\alpha_5 s^{(R)} s^{(1)} - 2\alpha_6 s^{(R)} s^{(1)} - 2\alpha_6 s^{(R)} s^{(1)} - \alpha_6 s^{(R)} s^{(1)} - \alpha_6 s^{(R)} s^{(1)} - 2\alpha_6 s^{(R)} s^{(1)} + 2\alpha_5 s^{(R)} s^{(1)} \\ & - d_{12}^4 - d_{11}^4) \theta_{0,yy}^{(1)} + (\alpha_2 + \alpha_3 + \alpha_4 + \alpha_5 + \alpha_7 + \alpha_9) s^{(R)} \theta_{0,yy}^{(1)} + (\alpha_3 + \alpha_2 + \alpha_4 + \alpha_6 + \alpha_{12}) s^{(R)} \theta_{0,yy}^{(1)} + R_{11}^4 + R_{12}^4 = 0 \end{aligned} \tag{A4}$$

$$\begin{aligned} \delta \theta_0^{(1)}: & (\alpha_4 + \alpha_5 + \alpha_7 + \alpha_2 + \alpha_3) s^{(R)} u_{0,xx}^{(1)} + (\alpha_4 + \alpha_5 + \alpha_2 + \alpha_3) s^{(R)} u_{0,xx}^{(1)} + (-a_{66}^4 - a_{11}^4 + \alpha_6 s^{(R)} s^{(1)} + \alpha_5 s^{(R)} s^{(1)}) \theta_{0,xx}^{(1)} \\ & + (\alpha_6 s^{(R)} s^{(1)} - a_{66}^4) \theta_{0,yy}^{(1)} + (\alpha_5 s^{(R)} s^{(1)} - a_{11}^4) \theta_{0,xx}^{(1)} + (2\alpha_5 + 2\alpha_4 + \alpha_3 + \alpha_7 + \alpha_9) s^{(R)} \theta_{0,xx}^{(1)} + (\alpha_3 + \alpha_2 + \alpha_4 + \alpha_6 + \alpha_{12}) s^{(R)} \theta_{0,xx}^{(1)} \\ & + \alpha_1 s^{(R)} \theta_{0,xx}^{(1)} + R_1^4 \theta_{0,xx}^{(1)} + (2b_{12}^4 + b_{21}^4 + 2\alpha_5 s^{(R)} s^{(1)} + \alpha_6 s^{(R)} s^{(1)} + 2\alpha_{12} s^{(R)} s^{(1)} + \alpha_6 s^{(R)} s^{(1)} - \alpha_5 s^{(R)} s^{(1)} - \alpha_6 s^{(R)} s^{(1)}) \theta_{0,xy}^{(1)} \\ & + (\alpha_5 s^{(R)} s^{(1)} + \alpha_6 s^{(R)} s^{(1)} - \alpha_6 s^{(R)} s^{(1)} + b_{11}^4) \theta_{0,xy}^{(1)} - (\alpha_4 + 2\alpha_5 + 2\alpha_4 + \alpha_3 + \alpha_7 + \alpha_9) s^{(R)} \theta_{0,xy}^{(1)} - (3\alpha_3 + 3\alpha_4 + \alpha_5 + 2\alpha_7 + \alpha_9 \\ & + 2\alpha_5 + \alpha_2) s^{(R)} \theta_{0,xy}^{(1)} - \alpha_1 s^{(R)} \theta_{0,xy}^{(1)} - IR_1^4 \theta_{0,xx}^{(1)} + (-\alpha_5 s^{(R)} s^{(1)} - \alpha_6 s^{(R)} s^{(1)} - \alpha_6 s^{(R)} s^{(1)} - 2\alpha_6 s^{(R)} s^{(1)} - 2\alpha_6 s^{(R)} s^{(1)} \\ & - 2\alpha_6 s^{(R)} s^{(1)} + 2\alpha_5 s^{(R)} s^{(1)} + 2\alpha_5 s^{(R)} s^{(1)} - d_{11}^4 - d_{12}^4) \theta_{0,xy}^{(1)} + (\alpha_2 + \alpha_3 + \alpha_4 + \alpha_5) s^{(R)} \theta_{0,xy}^{(1)} + (-d_{12}^4 \\ & + 2\alpha_5 s^{(R)} s^{(1)} - 2\alpha_6 s^{(R)} s^{(1)} - \alpha_6 s^{(R)} s^{(1)} - \alpha_6 s^{(R)} s^{(1)} - \alpha_6 s^{(R)} s^{(1)} - \alpha_6 s^{(R)} s^{(1)} - d_{11}^4) \theta_{0,xy}^{(1)} + (2\alpha_5 s^{(R)} s^{(1)} - 2\alpha_6 s^{(R)} s^{(1)} - 2\alpha_6 s^{(R)} s^{(1)} - d_{12}^4) \theta_{0,xy}^{(1)} \\ & + (\alpha_2 + \alpha_3 + \alpha_4 + \alpha_5 + \alpha_7 + \alpha_9) s^{(R)} \theta_{0,xy}^{(1)} + (\alpha_3 + \alpha_2) s^{(R)} \theta_{0,xy}^{(1)} + \alpha_1 s^{(R)} \theta_{0,xy}^{(1)} + (2\alpha_5 + 2\alpha_4 + \alpha_3 + \alpha_7 + \alpha_9 \\ & + \alpha_{12}) s^{(R)} \theta_{0,xy}^{(1)} + (\alpha_5 s^{(R)} s^{(1)} + \alpha_6 s^{(R)} s^{(1)} + \frac{1}{2} s^{(R)} s^{(1)}) \theta_{0,xx}^{(1)} + R_1^4 \theta_{0,xx}^{(1)} + R_{11}^4 + R_{12}^4 = 0 \end{aligned} \tag{A5}$$

$$\delta \theta_H^{(1)}: \quad \tilde{\mu}_1 \phi_{H,xx}^{(1)} + \tilde{\mu}_2 \theta_{H,yy}^{(1)} = 0 \tag{A6}$$

- The governing equations of motions of lower micro plate

$$\begin{aligned} \delta u_0^{(2)}: & -A_1^4 u_{0,xx}^{(2)} - A_1^4 u_{0,yy}^{(2)} + \alpha_1 s^{(0)} u_0^{(2)} + (2\alpha_5 + 2\alpha_4 + \alpha_3 + \alpha_7 + \alpha_9) s^{(0)} u_0^{(2)} + (\alpha_6 + \alpha_{12}) s^{(0)} u_{0,xy}^{(2)} \\ & + I_0^4 u_{0,xx}^{(2)} - (A_{12}^4 + A_{66}^4) v_{0,xy}^{(2)} + (\alpha_2 + \alpha_3 + \alpha_4 + \alpha_5) s^{(0)} v_{0,xy}^{(2)} + (\alpha_3 + \alpha_2 + \alpha_4 + \alpha_6 + \alpha_{12}) s^{(0)} v_{0,xy}^{(2)} \\ & - B_{12}^4 v_{0,xy}^{(2)} + (B_{12}^4 + 2B_{66}^4) w_{0,xy}^{(2)} - \alpha_1 s^{(1)} w_{0,xy}^{(2)} - (\alpha_2 + 3\alpha_3 + 3\alpha_4 + 2\alpha_5 + 2\alpha_7 + \alpha_9) s^{(1)} w_{0,xy}^{(2)} \\ & - (\alpha_4 + \alpha_2 + \alpha_6 + 2\alpha_7 + 2\alpha_{12}) s^{(1)} w_{0,xy}^{(2)} - I_1^4 w_{0,xy}^{(2)} + (-a_{11}^4 + \alpha_5 s^{(0)} s^{(1)}) \theta_{0,xx}^{(2)} + (-a_{66}^4 + \alpha_6 s^{(0)} s^{(1)}) \theta_{0,yy}^{(2)} \\ & + \alpha_5 s^{(R)} \theta_{0,xx}^{(2)} + (2\alpha_5 + 2\alpha_4 + \alpha_3 + \alpha_7 + \alpha_9) s^{(R)} \theta_{0,xx}^{(2)} + (\alpha_6 + \alpha_{12}) s^{(R)} \theta_{0,yy}^{(2)} + \alpha_6 s^{(R)} \theta_{0,yy}^{(2)} \\ & + R_1^4 \theta_{0,xx}^{(2)} + (-a_{11}^4 - a_{66}^4 + \alpha_6 s^{(R)} s^{(1)} + \alpha_5 s^{(R)} s^{(1)}) \theta_{0,xy}^{(2)} + (\alpha_2 + \alpha_3 + \alpha_4 + \alpha_5 + \alpha_7 + \alpha_9) s^{(R)} \theta_{0,xy}^{(2)} \\ & + (\alpha_3 + \alpha_2 + \alpha_4 + \alpha_6 + \alpha_{12}) s^{(R)} \theta_{0,xy}^{(2)} + N_{11}^4 + N_{12}^4 = 0 \end{aligned} \tag{A7}$$

